Interpretation of the unusual behavior of H_2O and D_2O at low temperatures: Tests of a percolation model

H. Eugene Stanley[a]

Center for Polymer Studies [b] and Department of Physics, Boston University, Boston, Massachusetts 02215

J. Teixeira

Laboratoire de Résonance Magnétique,[c] Ecole Supérieure de Physique et Chimie, 10, rue Vauquelin, 75231 Paris, France

(Received 8 January 1980; accepted 17 June 1980)

The unusual low-temperature behavior of liquid water is interpreted using a simple model based upon connectivity concepts from correlated-site percolation theory. Emphasis is placed on examining the physical implications of the continuous hydrogen-bonded network (or "gel") formed by water molecules. Each water molecule A is assigned to one of five species based on the number of "intact bonds" (the number of other molecules whose interaction energy with A is stronger than some cutoff V_{HB}). It is demonstrated that in the present model the spatial *positions* of the various species are not randomly distributed but rather are correlated. In particular, it is seen that the infinite hydrogen-bonded network contains tiny "patches" of four-bonded molecules. Well-defined predictions based upon the putative presence of these tiny patches are developed. In particular, we predict the detailed dependence upon (a) temperature, (b) dilution with the isotope D_2O, (c) hydrostatic pressure greater than atmospheric, and (d) "patch-breaking impurities"—for four separate response functions, (i) the isothermal compressibility K_T, (ii) the constant-pressure specific heat C_P, (iii) the constant-volume specific heat C_V, and (iv) the thermal expansivity α_P, as well as for dynamic properties such as (v) the transport coefficients self-diffusivity D_S and shear viscosity η, (vi) the characteristic rotational relaxation time τ_{ch}, and (vii) the Angell singularity temperature T_s. The experimentally observed dependence of these seven quantities upon the four parameters (a)–(d) is found in all cases to agree with the predicted behavior. The paradoxical behavior associated with the absence of a glass transition in pure liquid water is also resolved. Finally, we propose certain experiments and computer simulations—some of which are underway—designed to put the proposed percolation model to better tests than presently possible using available information.

I. INTRODUCTION

Angell and co-workers[1] have recently called attention to the fact that essentially all of the anomalous properties of water become even more striking when one supercools below the normal melting temperature T_m. Thus far no satisfactory physical mechanism underlying these unusual liquid phenomena has been found.

Recently, a new correlated-site polychromatic percolation model was proposed[2] that may be of relevance in providing some insight into the behavior at low temperature of H_2O and D_2O. It is of interest to explore the extent to which a given model can provide an explanation of a range of extremely anomalous phenomena. Accordingly, our purpose here is first to state rather more clearly the model itself in an attempt to remove certain rather serious ambiguities arising from the initial presentation. Among these are remarks that have led others to believe that the model is a member of a large class of "two-state" model systems, when in fact it is in fact a continuum model. Second, we shall make specific comparisons between the predictions of this model and experimental data on pure H_2O and D_2O at low temperatures. We shall see that the principal advantage of our approach is that it provides a single coherent mechanism capable of encompassing a wide range of anomalous phenomena for $T < T_m$, while in no way contradicting recent work of a much more quantitative nature that explains in detail some of the behavior for $T > T_m$. Moreover, it makes specific predictions concerning experimental data that are amenable to tests. In Sec. II, we review the correlated-site percolation model with emphasis on the nature of the assumptions involved in applying this simple "zeroth order" model to a system as complex as supercooled water and with emphasis on the degree to which this model is a natural extension of other models currently being developed for stable water ($T > T_m$). Section III analyzes two response functions: the isothermal compressibility and the constant-pressure specific heat. In Sec. IV other response functions are discussed, while in Sec. V we investigate the behavior of the entropy of supercooled water and the consequences for the glass transition paradox. Section VI is concerned with the time-dependent properties, such as the coefficient of self-diffusion and shear viscosity. Finally, in Sec. VII we discuss the sort of information that would be useful in providing more precise tests of the percolation model.

Appendix A attempts to resolve four frequently encountered confusions concerning the application of percolation concepts to liquid water, while Appendix B is designed to demonstrate that the numerical predictions of the present model are of the correct order of magnitude to be consistent with the observed experimental facts.

---

[a] John Simon Guggenheim Memorial Fellow, 1979–1980.

[b] Supported by grants from the AFOSR and ONR.

[c] Equipe de Recherche Associée 365 au CNRS.

 0021-9606/80/193404-19$01.00

II. MODEL

A. Background

Previous work aimed at elucidating the essential physical mechanism underlying the unusual behavior of *normal* water has been so well reviewed that we shall not attempt to cite every appropriate reference.[3-10] At the risk of oversimplifying a long and complex history, one might be tempted to state that models are conveniently partitioned into two broad categories: (a) mixture/interstitial models and (b) distorted hydrogen bond or "continuum" models.

Category (a) dates back to Roentgen's 1892 proposal that liquid water is a mixture of two basic components, a "bulky" icelike component and a comparatively less bulky "normal liquid."[11] Roentgen's essential idea has been developed and extended by many authors.[12-18] Although theories of category (a) have been successful in providing a physical mechanism for explaining a variety of anomalous properties of liquid water, there is an accumulating body of evidence that serves to render somewhat implausible the basic starting point of the approach. This evidence has been summarized quite convincingly by Kauzmann.[19]

Theories of category (b) date back almost 50 years to the proposal of Bernal and Fowler[20] that water forms a network that is more or less completely hydrogen bonded, with the effect of temperature being to distort the bonds (e. g., by "bending" them) rather than to formally "break bonds" as in mixture theories. The Bernal–Fowler idea has also been developed and extended by many workers[21-27] and does not suffer from many of the drawbacks of approach (a).

It is a fact that no theory belonging either to category (a) or category (b) has seriously addressed itself to the unusual behavior exhibited by supercooled water. In this paper we shall argue that the model proposed in Ref. 2 may be regarded as a natural extension (or refinement) of a "category (b) theory" that has as one advantage that it provides the first qualitative explanation of the supercooled phenomena and that it does so within a framework that applies equally to low-temperature water—i.e., the supercooled phenomena are found to be a natural extension of phenomena occurring just above T_m.

B. Considerations of connectivity

The model of Ref. 2 is rather abstract in its basic formulation, and the relevance to water is not at all apparent. For this reason, it is necessary to present this model rather more carefully—especially with a view to seeking to justify its possible relevance to elucidating the mechanisms underlying the unusual behavior of low-temperature H_2O and D_2O.

Despite the apparent lack of unanimity on the subject, many workers would agree with our starting point, namely, the hypothesis that "liquid water consists of a random hydrogen-bond network, with frequent strained and broken bonds, that is continually subject to spontaneous restructuring."[28] The mean number n_{HB} of hydrogen bonds per molecule depends, of course, on one's definition of hydrogen bond. However, for any reasonable definition, n_{HB} is sufficiently large that the oxygen atoms form an infinite connected network or "gel."[29] This hypothesis, which dates back some years, has recently received strong support from a decisive molecular dynamics calculation that concerned itself with the *bond* connectivity of liquid water and clearly demonstrated that the system is well above its bond percolation threshold.

Terms such as gelation and percolation refer not to the actual positions of the oxygen atoms, but rather to their connectivity. Since the water molecule is highly nonspherical, two water molecules can be bonded when separated by, say, 2.8 Å, while the same two molecules may not be bonded at a closer separation if their relative orientation is not appropriate. Accordingly, it is conventional when discussing gelation or percolation to refer to molecules not in the usual configuration space but rather in a topological or "connectivity" space: if two molecules are bonded, we draw a heavy solid line between them. If p_B is some measure of the probability of two nearby molecules to be hydrogen bonded, then we can make the obvious statement that at very low values of p_B the system breaks up into a set of dimers, trimers, etc. —all the networks are finite. However, above a well-defined gelation or percolation threshold, there exists—in addition to the networks of finite size—a single network that is infinite in spatial extent. Hence the statement that water is an infinite connected network or "gel" is simply the statement that p_B is above the bond percolation threshold.

It is perhaps necessary at this point to emphasize that neither percolation nor gelation phenomena have anything to do with the existence of a lattice. However, to the extent that a lattice affords a convenience for numerical calculations, virtually all quantitative work in both fields has been done either on (i) the "Cayley tree pseudolattice" (essentially a continuum model in which all closed loops are disallowed for the sake of mathematical simplicity) or on (ii) conventional two- and three-dimensional lattices reflecting the essential topological features of the system under consideration.

Similarly, we shall see that while the general formulation of the percolation model does not require the presence or even the concept of a lattice, the detailed numerical calculations that we have carried out thus far do indeed use a lattice—the ice I_h lattice—which is chosen to attempt to reflect the local tetrahedral symmetry of the water molecule. The fact that our numerical work *thus far* is for a lattice is one reason that the detailed quantitative predictions may be more useful in domains where the correlation length is not too large. The quantitative predictions may possibly begin to break down as the temperature of a system comes arbitrarily close to the apparent singularity at $T_s = -45\,^\circ\mathrm{C}$; most data supporting the possibility of such a singularity are restricted to T above about -30 or $-35\,^\circ\mathrm{C}$, and hence this possible shortcoming is not likely to be as serious as one might imagine it to be were there in fact data arbitrarily close to T_s.

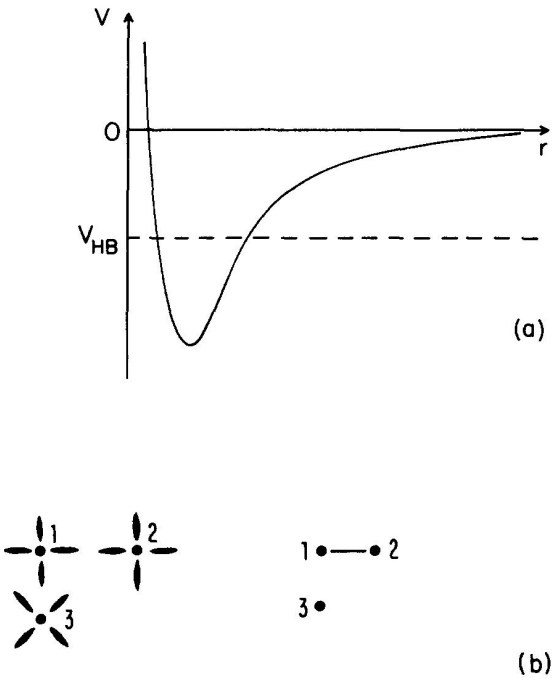

FIG. 1. (a) Schematic illustration of a water–water interparticle potential $V(r)$. The fact that the water molecule is highly asymmetrical implies that this curve depends not only on the water–water separation vector but also on the relative *orientation* of the two waters. Also shown is the concept of a cutoff parameter V_{HB}, as used extensively in molecular dynamics calculations. When the mutual energy of interaction is stronger than V_{HB}, we say that the two atoms have a bond between them; otherwise no bond is said to exist. This imposition of a discrete symmetry on a continuous physical function is discussed extensively in the text and also in Ref. 35. (b) Schematic representation of a subsystem of three H_2O molecules in "real space" and its representation in a "topological space" where only the two states of each possible hydrogen bond are taken into account. Note that it is quite possible for molecule 3 to be closer to molecule 1 (than molecule 2 is), yet the mutual interparticle potential $V(\mathbf{r})$ is below the threshold and hence no bond exists. Indeed, x-ray experiments in liquid water reveal the presence of roughly 4.5 molecules within a first-neighbor shell, yet for *realistic* choices of V_{HB}, at most four hydrogen bonds are formed (Refs. 29 and 39).

The model is perhaps best described in terms of the same considerations that have been used so successfully to date in molecular dynamics studies of liquid water.[7,30–34] Specifically, one begins by representing oxygen atoms as points in space, interacting one with another according to a potential that seeks to combine both the features of a normal liquid (Lennard–Jones type interactions) and the features unique to the water molecule (a strongly directional electrostatic interaction potential reflecting the local tetrahedral symmetry). This intermolecular potential is sketched in Fig. 1(a).

No matter how far apart two molecules are, they interact. We can state that two molecules are "hydrogen bonded" if their mutual interaction energy is less than some threshold V_{HB} [Fig. 1(a)]. We can thereby partition the oxygen atoms into different species: an oxygen is said to belong to species j if it is "hydrogen bonded" to j other oxygen atoms. Clearly there is a one-to-one relation between the threshold parameter V_{HB} and the mean number of bonds per molecule n_{HB}.[35]

The hydrogen bond framework so defined may be represented in a convenient "connectivity diagram" in which each molecule is represented by a point and each possible hydrogen bond by a line segment joining two points which are hydrogen bonded. It is important to emphasize that this connectivity diagram or "topological space" bears no obvious relation to configuration space. For example, if we consider two molecules that are hydrogen bonded, and then one is brought closer to the other but at the same time rotated, the bond may be "broken" in the sense that the mutual potential energy may become so large that it exceeds the threshold V_{HB} [Fig. 1(b)]. At low pressures, we can assume very simply that $p_B = \frac{1}{4} n_{HB}$, where n_{HB} is estimated by infrared or Raman spectroscopy techniques.[36,37] However, at high pressures, when the structure is deformed, p_B is certainly reduced even if n_{HB} is less affected. Indeed, the distortion of the hydrogen bond network under pressure can lead to an effective decrease of p_B, because it shifts a fraction of the populations of the bond energies across the threshold V_{HB}.

In view of the preceding paragraph, it is not surprising that the local symmetry of a given site in this topological space is tetrahedral. We shall make the assumption that the global symmetry of the connectivity diagram (or "topological space") is also roughly tetrahedral—specifically, that the connectivity properties are the same as those of the ice I_h lattice.[38] It is important to emphasize that this does not mean that we are assuming the oxygen atoms form a network that is the *same* as an ice I_h lattice, but only that the two systems are roughly equivalent topologically. Recent molecular dynamics calculations strongly support this assumption.[39]

C. Two features of the model

With the above preliminaries, we are now prepared to state the new features of the present picture and the reason that they may be expected to be of possible relevance to the low-temperature behavior of H_2O and D_2O.

One can ask two distinct levels of questions concerning the members of each species of oxygen atom. Question (i) is the question someone with a background in thermodynamics would ask, and indeed it has been asked by many workers previously: "What is the fraction f_j of oxygen atoms belonging to each species j?" Question (ii) is a question that has not to the best of our knowledge been asked before: "What is the detailed connectivity of each species?"

Questions concerning connectivity are the usual questions asked in percolation theory, except that we are asking these questions about oxygen atoms ("sites"), not about the hydrogen bonds ("bonds"). Since there are five different species of atoms, it is conventional to regard each species as a different color and hence the problem posed by question (ii) is called "polychromatic correlated-site percolation problem." Appendix A discusses in some detail the distinction between site and

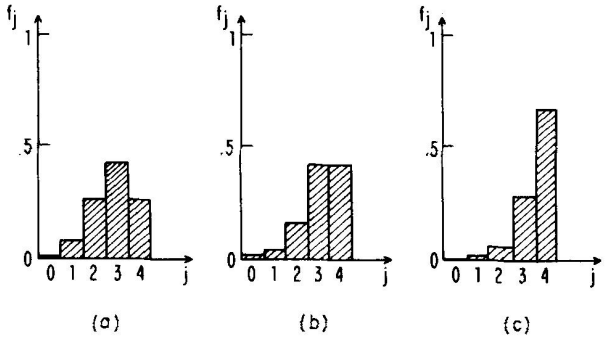

FIG. 2. Histograms based on Eq. (2.1) showing how the oxygen atoms are partitioned into five separate species, according as they have $0, 1, \ldots, 4$ intact hydrogen bonds. Parts (a), (b), and (c) correspond to $p_B = 0.7$, 0.8, and 0.9, respectively. The numerical values of $f_0 \ldots, f_4$ agree with the results of molecular dynamics calculations of Geiger (Ref. 39) provided one identifies p_B with $\frac{1}{4} n_{HB}$. The fact that for all values of p_B one obtains from Eq. (2.1) a simple *unimodal* distribution makes unequivocal the fact that the present model falls into category (b) (distorted hydrogen bond or continuum models) rather than category (a) (mixture/interstitial models), since category (a) models correspond to a bimodal histogram having local maxima at $j = 0$ (zero bonds) and $j = 4$ (four bonds).

bond percolation, as well as the distinction between random and correlated percolation.

A "zeroth order" answer to question (i) that is consistent with available information from detailed molecular dynamics studies (see Sec. VII A) is provided by the following two assumptions. First we assume that, for realistic choices of V_{HB}, at most a *minority* of oxygen atoms engage in more than four hydrogen bondings. This assumption is supported by molecular dynamics calculations, as well as being rather plausible considering the highly directional nature of the isolated H_2O molecule. Second, we assume that the hydrogen bonds are *randomly* intact with probability p_B and broken with probability $q_B \equiv 1 - p_B$.

These two assumptions permit us to answer question (i) unequivocally,

$$f_j = \binom{z}{j} p_B^j q_B^{z-j} \tag{2.1}$$

with $z = 4$, the maximum number of bonds per oxygen. The predictions of Eq. (2.1) are sketched in Fig. 2 for $p_B = 0.7$, 0.8, and 0.9, corresponding to $n_{HB} = 2.8$, 3.2, and 3.6. The dependence on p_B of f_0 is shown in Fig. 3 and compared with the molecular dynamics analysis data of Ref. 29 (see discussion in Sec. VII A).

Question (ii) may also be answered quantitatively—given the same two assumptions—by using the concepts of correlated-site percolation theory. As an illustration, consider the species-4 oxygen atoms. Although their total concentration $f_4 = p_B^4$ is determined by trivial considerations of random statistics, their *connectivity is far from random*. Rather, the positions of the species-4 oxygens are so strongly correlated that they tend to "clump" together, just as if there were an effective energy of attraction. This is a subtle and extremely surprising point, and it is perhaps useful to consider two examples to clearly demonstrate that species-4 oxygens can tend to clump together without being explicitly "driven" by an energy term.

Example 1. Suppose $p_B = 0.8$, which is well above the bond percolation threshold (about 0.4), so that the system includes an infinite random network. Consider a randomly chosen oxygen atom, and call it atom A (Fig. 4). If we know nothing about its four neighbors, then the probability that A is a member of the class of species-4 oxygen atoms is simply given by Eq. (2.1), since the probability is equal to the overall concentration $c = f_4 = p_B^4$,

$$\pi_4(4) = p_B^4 = 0.4096 . \tag{2.2a}$$

If, however, we know that one of the neighbors of A is species 4 and we are ignorant of the remaining three, then

$$\pi_4(3) = p_B^3 = 0.512 , \tag{2.2b}$$

a number 25% larger. If we know two neighbors are species 4, then

$$\pi_4(2) = p_B^2 = 0.64 , \tag{2.2c}$$

a number 25% larger still. If three neighbors are species 4, and we are ignorant of only one neighbor, then

$$\pi_4(1) = p_B^1 = 0.8 . \tag{2.2d}$$

Finally, if all four neighbors of atom A are species 4, then the site itself *must* be species A:

$$\pi_4(0) = p_B^0 = 1 . \tag{2.2e}$$

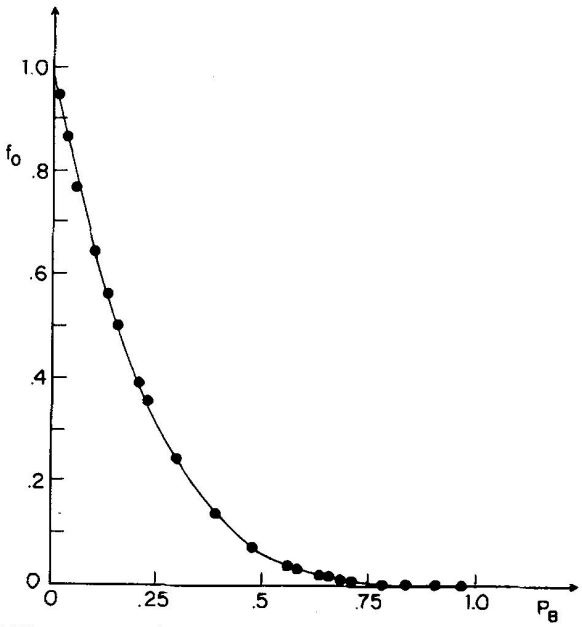

FIG. 3. Dependence on p_B of the fraction f_0 of oxygen atoms with zero intact bonds—as given by Eq. (2.1) (solid curve). The points represent three different molecular dynamics calculations on three separate systems (cf. Fig. 6 of Ref. 29 and Sec. VII A of the text), where we take $p_B = \frac{1}{4} n_{HB}$. The fact that the molecular dynamics data agree with the binomial distribution of Eq. (2.1) seems not to have been pointed out before [A. Geiger (private communication)].

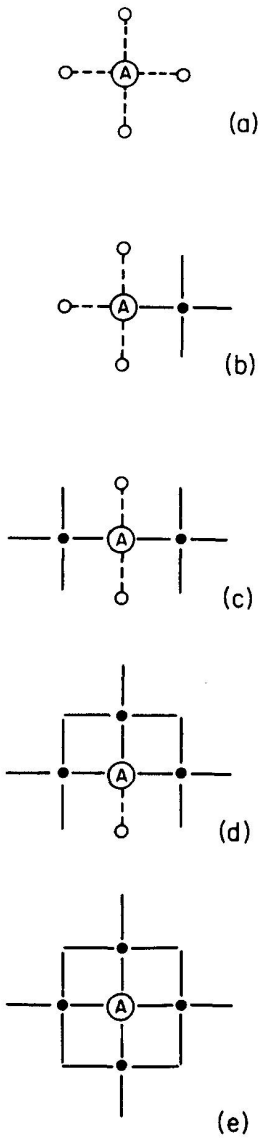

FIG. 4. Pictures corresponding to row 1 of Table I, illustrating the tendency of "black" sites (species-4 oxygens) to clump together. In (a), no "information" is known about the neighboring oxygens (i.e., $\tilde{S}=4$); hence the conditional probability $\pi_4(\tilde{S}=4)$ of site A being black is simply given by Eq. (2.2a). In (b)–(e), we assume progressively more information about the four neighbors ($\tilde{S}=3, 2, 1, 0$) and hence the conditional probability $\pi_4(\tilde{S})$ of site A being black increases Eqs. (2.2b)–(2.2e).

The above example clearly illustrates why the patches of species-4 oxygens are much more compact than would be the case if the species-4 oxygens were distributed at random with probability f_4. We can also illustrate this tendency to clump by means of computer simulation: Fig. 5(a) shows a random-site percolation simulation, while Fig. 5(b) shows the corresponding patch of species-4 oxygens in the "correlated-site" percolation problem that we are discussing. *For illustration purposes only*, the simulations shown are for a simple two-dimensional "lattice" with coordination number $z=4$, rather than for a three-dimensional "random network" appropriate to water. Analogous simulations have been carried out for three dimensions.[40]

The above remarks concern the probability of a randomly chosen atom to be species 4, given certain information about its immediate environment. Similar considerations apply for atom A to be species j, with $j=3$, 2, 1, or even 0; these results are elementary to obtain and are summarized in Table I.

Example 2. Example 1 concerns the tendency of black (species-4) oxygen atoms to clump, despite the assumption of random bond occupancy. The converse effect—the tendency of species-4 oxygens to appear infrequently in regions of white (non-species-4) oxygens—is also readily exemplified.

For example, we can easily calculate the probability W_1 that an oxygen atom A has four white neighbors; W_1 is the weight fraction of the random network or "gel" consisting of one-site patches. Clearly

$$W_1 = p_B^4 (1-p_B^3)^4 = c(1-c^{3/4})^4 , \tag{2.3a}$$

since p_B^4 is the probability of a randomly chosen atom to be black, $1-p_B^3$ is the probability that each of its four neighbors is not black, and $c=f_4=p_B^4$ is the concentration or "density" of black atoms.

If the atoms were randomly black, with probability c, then by the same reasoning we would have

$$W_1^R = c(1-c)^4 . \tag{2.3b}$$

The correlated and uncorrelated weight fractions W_1 and W_1^R are plotted in Fig. 6, and we see that

$$W_1 \leq W_1^R . \tag{2.3c}$$

In fact, for a concentration given by $c=0.4096$ (corresponding to $p_B=0.8$), we have

$$W_1 = 0.023 , \quad W_1^R = 0.050 . \tag{2.4}$$

Thus the effect of correlations is to reduce by more than half the probability of finding an isolated black atom.

Consistent with out intuition, the ratio W_1/W_1^R decreases still further as p_B increases in a nonlinear fashion. For example, suppose p_B increases 12.5%

TABLE I. Values of $\pi_j(\tilde{S})$ the *conditional* probability that a randomly selected site A is a member of species j, given the information that $(4-\tilde{S})$ of its neighbors are species-4 ("black dots"). Here $q=1-p$, and we drop the subscript B here for the sake of notational convenience. The discussion in the text concerns the S dependence of $\pi_4(\tilde{S})$ (cf. row 1). Also, when $\tilde{S}=4$, we find $\pi_j(\tilde{S})=f_j$—i.e., the probability that a randomly selected site is species j is equal to the overall concentration of species j (cf. column 1). Clearly $\tilde{S}$ is a measure of the "lack of information" or "entropy": when $\tilde{S}=0$, all four neighbors are black, while when $\tilde{S}=4$, nothing at all is known about the neighbors. Note that each element in this table is larger than the entry to its immediate right, corresponding to the obvious fact that $\pi_j(\tilde{S})$ decreases as $\tilde{S}$ decreases for fixed j. Note also that the sum of the probabilities of each species j is unity, regardless of S.

	$\tilde{S}=4$	$\tilde{S}=3$	$\tilde{S}=2$	$\tilde{S}=1$	$\tilde{S}=0$
$\pi_4(\tilde{S})$	p^4	p^3	p^2	p	1
$\pi_3(S)$	$4p^3q$	$3p^2q$	$2pq$	q	0
$\pi_2(\tilde{S})$	$6p^2q^2$	$3pq^2$	q^2	0	0
$\pi_1(\tilde{S})$	$4pq^3$	q^3	0	0	0
$\pi_0(\tilde{S})$	q^4	0	0	0	0
$\sum_{j=0}^{4}\pi_j(\tilde{S})$	$(p+q)^4$	$(p+q)^3$	$(p+q)^2$	$(p+q)$	1

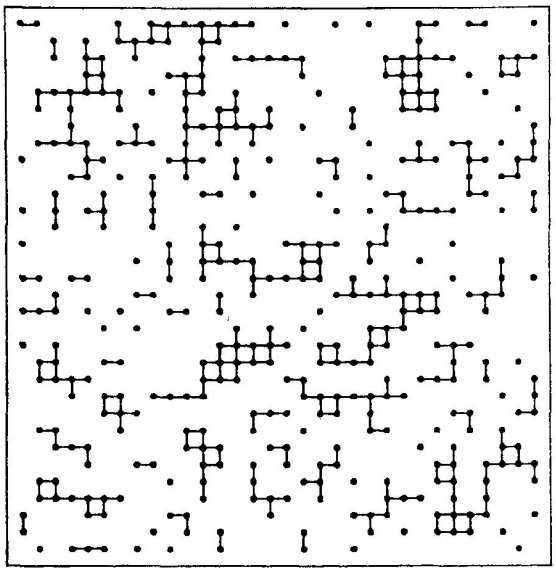

(a)

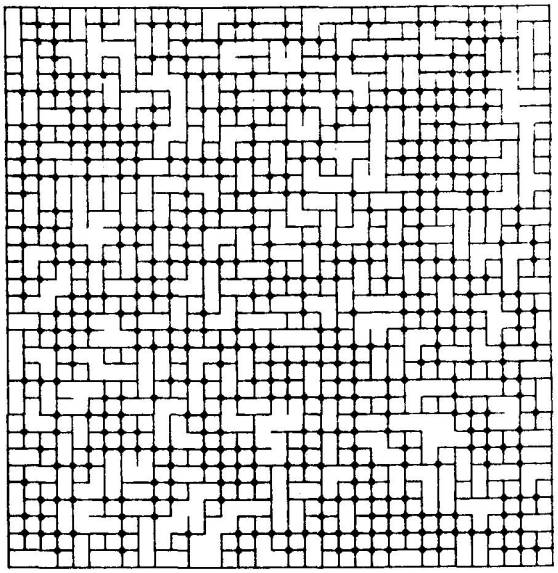

(b)

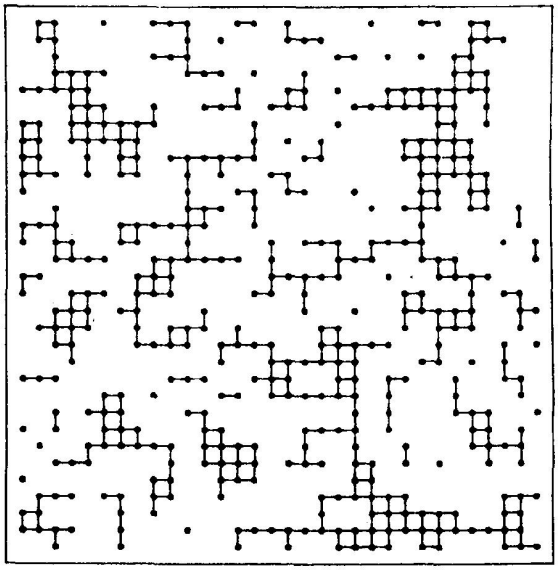

(c)

FIG. 5. Comparison of the site clusters in (a) random-site percolation and (b) correlated-site percolation at the same values of *site* concentration, 0.4096. In order to better visualize the clusters of four-bonded sites ("black dots") of part (b), we show in part (c) the *same* simulation only with all bonds removed and with a line segment placed between each nearest-neighbor pair of four-bonded site. Extensive simulations have been carried out for the ice I_h lattice; shown here is the square lattice for simplicity. These simulations of *finite* 32×32 lattices are consistent with the predictions of Eq. (2.4) that the number of 1-site patches is 1024 $W_1^R = 50.96$ in part (a) and 1024 $W_1 = 23.78$ in part (b) [cf. dashed line in Fig. 6].

from 0.8 to 0.9. The concentration of species-4 oxygen atoms increases 60% from $(0.8)^4 = 0.4096$ to $(0.9)^4 = 0.6561$, and from (2.3) we find

$$W_1 = 0.0035\,, \qquad W_1^R = 0.0092\,. \tag{2.5}$$

Clearly the effect of correlation is to reduce still further the probability of finding an isolated species-4 oxygen, as the ratio W_1/W_1^R has decreased by 21% from 0.4668 to 0.3856.

For $s>1$, one can calculate in a similar fashion the weight fractions W_s of isolated s-site patches of species-4 oxygens in our random network. For s large, this computation becomes increasingly difficult, but the important point is that the effect of correlations is to further minimize the weight fraction of isolated small s-site patches relative to the random case provided p_B is large.

For example, while we saw that the ratio W_1/W_1^R decreased 21% when p_B increased from 0.8 to 0.9, the corresponding ratio for two-site patches W_2/W_2^R decreases 50% (from 0.3986 to 0.2661) when p_B increases from 0.8 to 0.9. Thus, the effect of the correlations on the connectivity of the species-4 atoms is even larger for $s=2$ than for $s=1$.

III. BEHAVIOR OF K_T AND C_P AS FUNCTIONS OF TEMPERATURE, PRESSURE, AND "IMPURITY" CONCENTRATION

Thus far we have described a model that is based on the premise that water consists of an infinite hydrogen bonded network with many strained and broken bonds. The existence of broken bonds permits us to partition the oxygen atoms into five different species, depending on the number of intact bonds incident upon a given oxy-

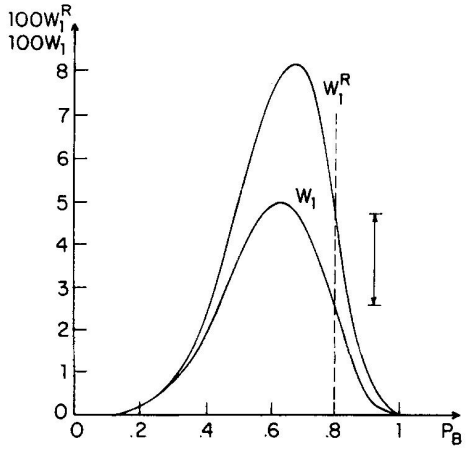

FIG. 6. Dependence on the parameter p_B of W_1, the "weight fraction" of oxygen atoms belonging to one-site clusters. Shown for comparison is the corresponding function W_1^R for random-site percolation. The ratio W_1/W_1^R decreases from unity (at $p=0$) to $(3/4)^4=0.316$ as p_B approaches unity. Recent molecular dynamics data (Ref. 39) agree (within the error bars) with the predictions for W_1, despite the fact that the W_1 is obtained for an ice I_h lattice while the molecular dynamics calculations are for a continuum system. Analogous plots (with analogous agreement) can be made for $W_2, W_3, \ldots$; the results of a detailed comparison with molecular dynamics will be published elsewhere.[39] The vertical arrow indicates the difference in the number of one-site clusters expected in Figs. 5(a) and 5(c), and the prediction may be borne out by direct counting.

gen. Percolation theory concerns itself with the *connectivity* of the members of each species. We saw in Sec. II that the connectivity properties were those of a *correlated* system; in particular, the species-4 atoms tend to "clump" together, forming patches of the infinite hydrogen bonded network that are in general larger and less ramified than the clusters found in a random-site percolation problem.

In the remainder of this paper, we shall discuss the possible relevance of this simple model to the unusual behavior of liquid H_2O and D_2O at low temperature.

A. Density fluctuations

The thermodynamic response function K_T, the isothermal compressibility, is defined through the relation

$$\bar{\rho}K_T \equiv \left(\frac{\partial \bar{\rho}}{\partial P}\right)_T , \tag{3.1a}$$

where $\bar{\rho}$ is the mean "global" mass density and P is the pressure. Statistical mechanical considerations[41] permit one to relate K_T to the ensemble average of the density fluctuations, $\delta\rho \equiv \rho - \bar{\rho}$,

$$K_T(k_B T\bar{\rho}^2/V) = \overline{(\delta\rho)^2} , \tag{3.1b}$$

where k_B is the Boltzmann constant. As T decreases, we expect the density fluctuations to also decrease. Indeed, for most liquids, K_T decreases with decreasing temperature. For H_2O, this is also true at high T, but for $T<46\,^\circ$C, K_T actually increases as T decreases. Moreover, Frank has noted that the magnitude of the density fluctuations is roughly twice as large for normal water as for most liquids.[42]

To explain these unusual phenomena, we consider the effect of the "patches" of species-4 oxygens in the hydrogen-bonded network. Suppose, e.g., that a Maxwell demon is sitting in a species-4 patch. Certainly the *local* density seen by him should be smaller than the overall *global* density of the infinite hydrogen-bonded network. Accordingly, there is an additional increase in density fluctuations due to the presence of the small patches, accounting for Frank's observation; we can quantitatively estimate the magnitude of this contribution, and this calculation is carried out in Appendix B, Sec. A. Moreover, the density fluctuations are enhanced by the fact that the spatial positions of the species-4 atoms are not random, but are correlated—just as the density fluctuations (and hence K_T) of a van der Waals gas are enhanced relative to an ideal noninteracting gas.

Thus in addition to the "normal" behavior in which decreasing temperature *decreases* the density fluctuations, there is an "anomalous" behavior caused by the fact that decreasing temperature increases the characteristic size of the small patches and hence *increases* the density fluctuations. The result of both effects is that at high temperatures K_T decreases with decreasing T, but at low temperatures K_T begins to increase.[43,44] If K_T were due mainly to these two physical mechanisms, then we could state that they exactly compensate or balance at $T=46\,^\circ$C, the "temperature of minimum compressibility."[43]

For D_2O, p_B is larger than for H_2O at the same value of T (cf. Appendix B, Sec. B). Hence the mean patch size is larger and $\overline{(\delta\rho)^2}$ increases. The foregoing considerations predict that for D_2O, the compressibility should be larger—and this is indeed observed to be the case.[45] In fact, the compressibility minimum for D_2O should occur at a temperature rather higher than 46 °C. Corresponding to the minimum in the isothermal compressibility is a maximum in the velocity of longitudinal sound waves v_s that is related to the adiabatic compressibility through $v_s^2=(\bar{\rho}K_S)^{-1}$; v_s has been measured quite accurately both in ultrasonic and hypersonic frequency domains.[46-49] This maximum increases from 73 °C for H_2O to 79 °C for D_2O.[50]

As noted in Sec. II B, p_B decreases with hydrostatic pressure P. Hence the patch size also decreases, and we predict that the effect of hydrostatic pressure should be to decrease K_T. Again this is found to be the case.[45] In fact, for pressures of the order of 1–2 kbars, K_T varies very little with T at low T.[45]

Suppose now that we add a second component or "impurity." If the impurity molecule can form hydrogen bonds with water molecules (e.g., H_2O_2, N_2H_4, or C_2H_5OH), then we term these "patch-breaking impurities."[51] When a water molecule belonging to a patch is replaced by such an impurity, we expect that the local density of the patch will increase (i.e., become more like the rest of the network), and hence the anomalous contribution to the total compressibility will become

smaller. Note that we might expect an "amplification mechanism" for the effect of impurities: relatively few molecules of a second component should decrease the compressibility considerably.

This prediction can be tested by comparing with experimental data. For example, extremely accurate measurements of the effect on K_S of the "patch-breaking impurity" ethanol have recently been carried out.[51] Since the compressibilities for the two pure systems are related by

$$K_T(C_2H_5OH) > K_T(H_2O) , \tag{3.2}$$

one might have expected that adding ethanol to pure water would serve to increase the measured compressibility. In fact, the reverse occurs: the compressibility is significantly decreased, by an amount well outside the experimental accuracy.[51]

A second possibility is that the impurity cannot form hydrogen bonds with water molecules (e.g., Ar, Ne, or CH_4). Such an impurity is less likely to displace a water molecule belonging to a patch than a water molecule in the rest of the "gel." Hence we might anticipate that the compressibility should increase.

In summary, the presence of many tiny correlated low-density patches of the infinite random hydrogen-bonded network correctly predicts the following four classes of observed phenomena.

(a) K_T increases with decreasing temperature at low temperatures, in sharp contrast with the behavior of most liquids, for which K_T decreases monotonically with decreasing T.

(b) $K_T(T, P)$ for D_2O is larger than $K_T(T, P)$ for H_2O at the same values of temperature and pressure, and the temperature of minimum compressibility increases.

(c) For pressures greater than atmospheric, $K_T(T, P)$ decreases and the low-temperature anomaly becomes progressively weaker.

(d) K_T decreases in the presence of a "patch-breaking" impurity.

B. Entropy fluctuations

The thermodynamic response function C_P, the constant-pressure specific heat, is defined through the relation

$$T^{-1}C_P \equiv \left(\frac{\partial \bar{S}}{\partial T}\right)_P , \tag{3.3a}$$

where $\bar{S}$ is the mean "global" entropy. Statistical mechanics relates C_P to the ensemble average of the entropy fluctuations $\delta S \equiv S - \bar{S}$,[52]

$$k_B C_P = \overline{(\delta S)^2} . \tag{3.3b}$$

Again, imagine a Maxwell demon situated in the center of a species-4 patch. Clearly the *total* entropy he sees will be considerably reduced, due to the local increase in spatial order in the interior of the patch. Appendix B, Sec. C discusses the relative magnitude of the density and entropy fluctuations (K_T vs C_P).

Thus the presence of correlated patches of *local* spatial order predicts the following four additional classes of phenomena that are analogous to the four discussed in Sec. 3.1 for K_T.

(a) C_P for H_2O increases at very low temperatures.[53–57]

(b) $C_P(T, P)$ for D_2O is larger than $C_P(T, P)$ for H_2O at the same values of temperature and pressure.[56,58]

(c) Under pressures greater than atmospheric, $C_P(T, P)$ decreases and its temperature dependence is less sharp.[58]

(d) $C_P(T, P)$ decreases in the presence of "patch-breaking" impurities.[57]

IV. BEHAVIOR OF THE REMAINING RESPONSE FUNCTIONS WITH T, P, AND IMPURITIES

In Sec. III, we discussed two of the more commonly studied response functions, K_T and C_P, as T, P, and isotope "impurity" concentrations are systematically varied. We saw that the presence of correlated low-density and locally "ordered" patches at low temperatures and pressures in pure water correctly predicts a wide variety of experimental phenomena.

In the present section, we discuss the additional response functions that are customarily measured in water.

A. Constant-volume specific heat

Since an essential physical feature of the tiny patches of four-bonded oxygens is the fact that they have a local density slightly smaller than the global density $\bar{\rho}$, it follows that any function measured at constant volume would be predicted to have no anomaly. This prediction can be tested on the constant-volume specific heat, which may be obtained from experimental data on C_P, α_P, and K_T using the thermodynamic identity

$$C_V = C_P - TV\alpha_P^2/K_T , \tag{4.1}$$

where

$$\alpha_P \equiv -\bar{\rho}^{-1}\left(\frac{\partial \bar{\rho}}{\partial T}\right)_P \tag{4.2}$$

is the coefficient of thermal expansion or "thermal expansivity." The prediction is indeed borne out by the data[1,56]: C_V remains almost constant down to the lowest temperatures on which reliable data exist.

B. Thermal expansivity

For most liquids, the thermal expansivity α_P defined in Eq. (4.2) varies only weakly as T decreases, so that the mean "global" density $\bar{\rho}(T)$ increases roughly linearly in T as the temperature is decreased. However for pure H_2O at atmospheric pressure, $\bar{\rho}(T)$ increases much less fast than linear (α_P is smaller) and $\alpha_P(T)$ is far from constant even for very large T. This behavior is thus just as if there were (in addition to the "normal" temperature-independent contribution) an "anomalous" contribution that is negative and that increases in absolute value rapidly with decreasing temperature.

The normal and anomalous contributions to α_P cancel precisely at the "temperature of maximum density," T_{MD}. For pure H_2O at atmospheric pressure, $T_{MD} = 4\,^\circ C$.

The fluctuation relation analogous to (3.1b) and (3.3b) is that α_P is proportional to the cross-fluctuations of volume and entropy.

$$\alpha_P \equiv \frac{1}{\bar{V}}\left(\frac{\partial \bar{V}}{\partial T}\right)_P \propto \langle \delta V \delta S \rangle . \tag{4.3}$$

For most liquids, when there is a local volume fluctuation with a positive δV, there is a corresponding *increase* in the local entropy ($\delta S > 0$). However, for the patches in question, $\delta S < 0$ when $\delta V > 0$, so that there is indeed an anomalous *negative* contribution α_P^A to the thermal expansivity.

The dependence of the response function $\alpha_P(T, P)$ on T, P, and "impurity" concentration may be readily interpreted in terms of the discussion presented in Sec. II. As T decreases, p_B increases and the concentration f_4 of four-bonded oxygens varies as p_B^4, thereby providing an "amplification mechanism" that is necessary if the density is to vary in a nonlinear fashion with T. The predictions for α_P analogous to those presented in Secs. III A and III B for K_T and C_P include the following.

(a) For pure H_2O, the anomalous contribution should increase in absolute magnitude, increasingly rapidly as T is decreased, so that the density should continue to decrease as T is lowered below T_m in a highly nonlinear fashion as predicted by the $f_4 = p_B^4$ "amplification mechanism"; this phenomenon is indeed confirmed experimentally.[44,59,60]

(b) For D_2O, we can make three predictions. First, the anomalous contribution should be larger than for H_2O; hence $\alpha_P(T, P)$ for pure D_2O should be smaller (more negative) than $\alpha_P(T, P)$ for H_2O at the same values of temperature and pressure.[56,57] Second, T_{MD} is predicted to be larger for D_2O than for H_2O; in fact, $T_{MD} = 11\,^\circ C$ for D_2O.[44] Third, the density maximum should also become sharper for D_2O, and this is found to be the case.[60,61]

(c) For pressures greater than atmospheric, the anomalous contribution to $\alpha_P(T, P)$ decreases in absolute value, so that $\alpha_P(T, P)$ is closer to its "normal fluid" value. Detailed measurements on the pressure dependence of α_P confirm this prediction.[62] Moreover, T_{MD} is predicted to decrease sharply with pressure, and this is also verified experimentally.[61] The density maximum should become less sharp under pressure (the opposite effect from D_2O), and the data also confirm this prediction.[60,61]

(d) The effect of a "patch-breaking impurity" on $\alpha_P(T, P)$ should be qualitatively similar to the effect of pressure, and this is found to be the case.[51]

V. PARADOXICAL BEHAVIOR ASSOCIATED WITH THE GLASS TRANSITION

"Normal liquids" that undergo a glass transition at some temperature T_g are frequently characterized by a

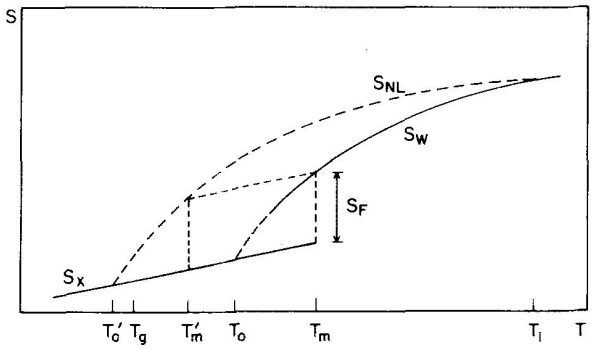

FIG. 7. Schematic illustration of the dependence on temperature of the entropy S_W of liquid water and the presumed entropy S_{NL} that waterlike particles would have were there no hydrogen bonds. Also shown is the entropy S_x of crystalline ice I_h. Note that $S_W(T)$ intersects $S_x(T)$ at a temperature T_0 that is well above the putative glass transition temperature T_g (see discussion in Sec. VI). The parameter T_m' is the melting temperature to be expected for the "normal liquid" if the entropy of fusion S_F were unchanged from its value in water (of course, this is only roughly true); that T_m' turns out to be about 100 °C lower than T_m is consistent with Pauling's analysis (Ref. 67).

liquid-state entropy $S_{NL}(T)$ that approaches their crystal-state entropy $S_x(T)$ at a temperature T_0' that is generally found to be slightly smaller than T_g (cf. Fig. 7). In short, the "entropy catastrophe" that would occur as T is decreased toward T_0' is prevented by the glass transition.[55,63,64] This phenomenon is sometimes called the Kauzmann paradox.

No glass transition has ever been observed in liquid water, even at remarkably high quenching rates; glassy water has, of course, been obtained from the vapor phase but never from the liquid phase.[65] However, if relatively small amounts of a second component are added to pure water, then a glass transition is observed at a temperature $T_g(x)$ that depends roughly linearly on the mole fraction x of the second component.[64] If one extrapolates the $T_g(x)$ data to $x = 0$ (i.e., pure water), then one would predict that $T_g = 140$ K for pure water.[1,64] The same estimate may be obtained by independent methods.[66] Hence one might imagine that $S_W(T)$, the entropy of liquid water, would approach $S_x(T)$, the entropy of ice, at a temperature T_0 just below 140 K. The anomalously large value of $C_P(T)$ for pure H_2O implies $T_0 = 208$ K,[55] a value considerably larger than 140 K. In fact, it is impossible by any reasonable extrapolation to reach 140 K without exhausting the entire entropy of fusion S_F, since

$$\Delta S(T) \equiv \int_T^{273} [C_P(T') - C_P^{ice}(T')]\, d(\ln T') \tag{5.1}$$

exceeds S_F for $T < T_0$.

In the proposed percolation model, these anomalous results can be understood because of the presence of structured ("low-entropy") patches of the random hydrogen bonded network that serve to decrease the entropy below what it would be were there no "patches." That is, the growth of structured patches in liquid water creates an irreversible situation tending toward crystal-

lization, and formation of glassy state would not be expected.

The above argumentation—albeit somewhat intuitive—can be put to experimental test (see also the discussion in Appendix B, Sec. D).

(a) Dilution of pure water with "patch-breaking impurities" should restore the glass transition; this is indeed observed, as noted above.[64]

(b) A smaller percentage of impurity should be required to restore the glass transition if the experiment is carried out at pressures greater than atmospheric. This prediction has also been confirmed in recent unpublished results.[65]

(c) For D_2O, a higher percentage of impurity should be required to restore the glass transition; this prediction remains to be tested by experimentation, to the best of our knowledge.

(d) Pauling[67] considered the sequence of T_m values for the isoelectronic sequence of hydride molecules H_2Te, H_2Se, H_2S, and H_2O. Since the latent heat of fusion TS_F is comparable for all members of the sequence ($S_F \cong 5.3$ cal mol^{-1}K^{-1} for H_2O), we could infer from Fig. 7 that, were there no hydrogen bonds present in H_2O, T_m would occur at a temperature T_m' that is of the order of magnitude of 100 K lower than the observed T_m for H_2O. This is in fact the same conclusion reached by Pauling from simple extrapolation of the T_m values for the isoelectronic sequence. Hence we would predict that T_m is increased by D_2O and decreased by pressure or the addition of patch-breaking impurities; this is indeed found to be so.

VI. DYNAMIC BEHAVIOR OF H_2O AND D_2O AS A FUNCTION OF TEMPERATURE, PRESSURE, AND "IMPURITY" CONCENTRATION

Measurements of the many time-dependent properties of low-temperature water reveal a number of anomalies that are readily interpreted in the present picture. The dynamical processes occurring in liquid water are characterized by the fact that hydrogen bonds are breaking and forming with a typical characteristic time τ_{HB} that is of the order of 10^{-12} sec.[68] Simulations such as those displayed in Fig. 5 hence correspond to "snapshots" of water with a shutter speed that is much shorter than τ_{HB}. Thus, even though water is believed to be a hydrogen-bonded random network, well above its percolation or "gelation" threshold, it cannot support a static or low-frequency shear stress like a common gel.

There are two possible interpretations of the dramatic decrease in transport at low temperatures and the anomalous pressure behavior. The first is very rough: we simply note that if the highly structured local patches of the infinite connected network are responsible for the dominant physical mechanism, then since $f_4 = p_B^4$ increases rapidly with decreasing temperature, we would expect the following predictions.

(a) The shear viscosity η should increase much faster at low temperatures than would be anticipated from the simple Arrhenius dependence found at high temperatures and for other liquids. This is indeed observed.[69,70]

(b) The coefficient of self-diffusion, D_s, should decrease much faster at low T than would be predicted by extrapolation of its high-temperature values, which are linear when plotted as $\log D_s$ against $1/T$. This is also observed.[71,72]

(c) The characteristic relaxation times τ_{ch} should increase rapidly as T is lowered.[73–75]

(d) For D_2O, f_4 should be larger than for H_2O, and hence $[D_s]^{-1}$, τ_{ch}, and η should be larger also.[76,77]

(e) Pressure and "patch-breaking impurities" should serve to decrease η, $[D_s]^{-1}$, and τ_{ch}. Indeed, the observed pressure dependence of η and D_s has been referenced frequently as being among the more bizarre properties of low-temperature water.[78]

Conversely, one might regard transport as arising from a "mobile" fraction F_M, which might be some weighted combination of the form

$$F_M = Af_0 + Bf_1 \,. \tag{6.1}$$

The foregoing conclusions (a)–(e) follow. In Appendix B, Sec. E we carry through an illustrative calculation using this possibility and demonstrate that quantitative agreement with experimental data over quite a wide range of temperature may be obtained.

VII. DISCUSSION

In the foregoing, we have discussed a variety of experimental data on H_2O and D_2O as function of temperature T, pressure P, and mole-fraction x of "patch-breaking impurity." We have seen that the general dependence of various measured functions on T, P, and x is consistent with the predictions of a "correlated percolation" model, in which one regards low-temperature water as being a random hydrogen-bonded network, local patches of which are four-coordinated. We must emphasize again that when looking at the bond connectivity problem, water appears as a large macroscopic space-filling hydrogen bond network (as expected from continuum models of water). It is only when looking at the four-bonded oxygens that water takes on certain clustering features—the clusters being not isolated "icebergs" in a sea of dissociated liquid, but rather embedded in a highly connected network or gel.

In Appendix B, we shall see that this picture of low-temperature water is not only qualitative, but also quantitative in that the sorts of numbers needed for agreement with experimental data are reasonable.

Before concluding, it is perhaps appropriate to discuss future tests, several of which have been initiated subsequent to the initial proposal of the correlated-percolation model. These tests naturally partition themselves into two categories: (i) those based on highly sophisticated methods of computer simulation (Monte Carlo and molecular dynamics), and (ii) those based on laboratory experimentation.

A. Computer simulation

In molecular dynamics, one is able to obtain a wealth of microscopic information about a given system provided one can choose an appropriate effective interaction potential. The considerations involved in the selection of an effective potential that best corresponds to the rich and subtle physics of the water molecules have been described in considerable detail elsewhere.[7,34]

The possibility of making detailed quantitative comparisons between the present model and computer simulations offers the opportunity of testing the validity of the picture put forth in Sec. II.

In particular, the computer simulation methods offer the possibility of clearly distinguishing between the positions of molecules in real three-dimensional space and their connectivity in the "topological space," since it is possible to consider the detailed connectivity patterns that emerge from a given analysis.[29,39]

Here we consider three aspects of the model that may be compared with the results of computer simulations.

(a) *Water is well above its bond percolation threshold.* The reason that the model requires p_B to be above the bond percolation threshold p_B^c is that for an ice-I_h lattice, the density of four-bonded oxygen atoms is p_B^4 by (2.1), and $p_B^c = 0.39$ is very small.[79] In fact, for $p_B < 0.39$, almost all patches of species-4 oxygens are extremely small. To see this, we note from Eq. (2.3a) that the weight fraction of isolated species-4 (four-bonded) molecules at $p_B = 0.39$ is $W_1 = 0.018$, while the total concentration of species-4 oxygens is, from (2.1), $f_4 = 0.023$; i.e., 83% of the species-4 oxygens are single isolated patches. One can also calculate the weight fraction of black sites belonging to two-site patches, with the result

$$W_2 = 4p_B^7(1-p^3)^6 \ . \tag{7.1}$$

For $p_B = 0.39$, $W_2 = 0.004$. Hence $W_1 + W_2 = 0.022$, almost the total concentration of the species-4 oxygens. Thus we see that at or below the bond percolation threshold, more than 96% of the species-4 oxygens belong to one-site or two-site patches. Hence a prerequisite for the validity of the correlated-percolation model of Sec. II is that water be well above the bond percolation threshold. This requirement has recently been convincingly demonstrated by molecular dynamics computer simulation: for any chemically reasonable definition of "hydrogen bond," a system of waterlike particles interacting through an ST2 potential exceeds its percolation threshold.[29,39]

(b) *The concentrations of each of the five species of oxygens conforms to Eq.* (2.1). Although the model presented in Sec. II does not of itself require that the bonds form randomly, the detailed numerical calculations are greatly facilitated if we can make this simplifying assumption. To the extent that the bonds are random, Eq. (2.1) should hold if V_{HB} is chosen so that few molecules have more than four intact bonds. Of course, nothing in nature is truly random, and hence it is important to obtain some measure of how serious an approximation (2.1) is in fact.[80]

In order to compare the predictions of (2.1) with molecular dynamics computer simulations, it is necessary to make a correspondence between the parameter p_B (the probability that a randomly chosen bond is intact) and the molecular dynamics parameter V_{HB} that corresponds to the definition of a hydrogen bond [cf. Fig. Fig. 1(a)]. There is a 1:1 correspondence between V_{HB} and n_{HB}, the number of hydrogen bonds per oxygen atom; clearly as the cutoff value for bonding, V_{HB}, increases (i.e., becomes more permissive), n_{HB} also increases. Except for extremely large values of V_{HB}, $n_{HB} \leq 4$ and we can plausibly compare plots of f_j vs p_B from Eq. (2.1) with molecular dynamics results for f_j vs n_{HB} with $n_{HB} = 4p_B$.

Geiger *et al.*[29] calculated f_0, the concentration of unbonded water molecules, as a function of n_{HB} for three different systems: (I) 216 water molecules at 11 °C and normal pressure, (II) 216 water molecules at 98 °C and high density, and (III) 1728 molecules at −1 °C. For all three systems, they find the *same* dependence of f_0 on n_{HB}. The fact is that the molecular dynamics results agree with the dependence predicted by Eq. (2.1) to a remarkable degree: a plot of f_0 vs $4p_B$ can be superposed on Fig. 6 of Ref. 29, with a maximum discrepancy of ±0.01 (cf. Fig. 3).

The concentrations f_j of the other four species of oxygen atoms are not tabulated in Geiger *et al.* However Stillinger[81,82] gives all five f_j for one particular value of n_{HB}, $n_{HB} = 2.3$ (corresponding to $p_B = 0.575$). Equation (2.1) predicts that $(f_0, f_1, \ldots, f_4)$ take on the values 0.033, 0.177, 0.358, 0.323, and 0.109; all five numbers are in excellent agreement with molecular dynamics results (Fig. 5 of Ref. 81).

Very recently, Geiger[39] has calculated the concentrations f_j of all five species for system (I). He finds excellent agreement with the predictions of Eq. (2.1) for the entire range of n_{HB} (cf. Fig. 2).

(c) *The connectivity of the oxygen atoms conform to the predictions of correlated-site percolation theory.* Geiger has also calculated as a function of n_{HB} the weight fractions $W_s(n_{HB})$ of four-bonded oxygens belonging to a s-site cluster, for $s = 1, 2, 3, \ldots$. The agreement with the W_s calculated for the model of Sec. II is quite remarkable and will be reported at length elsewhere, along with detailed comparisons of the other cluster properties such as mean cluster size, radius of gyration, and "total number of patches." That the molecular dynamics calculations should agree with the detailed microscopic predictions of correlated-site percolation theory provides one of the more striking confirmations of the utility of the present picture.

B. Experimental tests

The model developed in Sec. II predicts that all properties of water can be related—to zeroth order—to a single parameter p_B and its dependence on temperature, pressure, "patch-breaking" impurity concentration, and isotope D_2O. Clearly it would be highly desirable to obtain a reliable estimate for p_B, and a combined experimental and theoretical effort toward this end is under way.

A key feature of the present model is that the striking phenomena observed in the supercooled region ($T < T_m$) are basically an analytic extension of the behavior observed for $T > T_m$. Accordingly, it is important to ascertain that the parameter p_B varies smoothly as T decreases deep into the supercooled region. There are many indications that this is the case.[1,83,84] If p_B can be measured quantitatively, then this matter may be resolved. Accordingly, efforts are under way to theoretically interpret spectroscopic data quantitatively in terms of p_B.

One prediction of the foregoing analysis concerns the behavior of water under pressure or in the presence of patch-breaking impurities. Specifically, we predict a continuous evolution toward the behavior of a "normal" assoicated liquid. Extremely detailed data with a fine "mesh" of presure and/or impurity values are required to fully test this prediction. Very recently such data have been obtained for the specific heat,[57] and the agreement with the predictions of the model is quite encouraging. Such data are also being obtained for the adiabatic compressibility (from Brillouin spectroscopy), and again the agreement is excellent.[51]

Conversely, the detailed effects of D_2O dilution should be studied in more detail—with remarkably few exceptions,[77] data exist only at the extremes of zero D_2O and 100% D_2O.

A variety of new experiments concerning dynamic properties are planned or else under way. Quasielastic neutron scattering experiments are in progress,[85] and these should be extremely useful since the width of the central peak (centered about $\omega = 0$) is a direct measure of diffusive motion.[86] Such experiments have previously been carried out only for comparatively high temperatures.[87,88] Moreover, because the molecular dynamics calculations give such striking agreement with the static properties, it is perhaps appropriate to consider extending these calculations to the point that they can provide detailed dynamic information.

Of course, the direct observation of patches of four-bonded oxygen atoms would provide a convincing proof for the essential correctness of the model. This goal is not likely to be attained, however, since it is quite clear from detailed Monte Carlo and molecular dynamics calculations[39,89] that the clusters are extremely small, even at the lowest attainable temperatures. The mean hydrogen bond lifetime is also extremely short (probably less than 10^{-12} sec). Bosio is in the process of making detailed measurements at extremely low temperatures of small-angle x-ray scattering,[90] and a corresponding project exists for small-angle neutron scattering.[91] Neutron scattering from supercooled water under pressure is also under way.[92]

C. Possible singularity near −45 °C

A particularly intriguing open question is the possibility of a true singularity in both static (thermodynamic) and dynamic (transport) quantities at some temperature T_s, with T_s roughly 228 K or −45 °C for pure H_2O when $P = 1$ bar.[1] There is a rather impressive quantity of experimental evidence supporting this possibility. However, none of the evidence pertains to data for $T < 237$ K, so that the minimum value of the reduced temperature $\epsilon \equiv (T - T_s)/T_s$ is roughly 0.05. This is in marked contrast to conventional critical point experiments, where one can nowadays make measurements so close to the critical point that ϵ is as small as 10^{-6}. It is very tempting to speculate that perhaps the phenomena that appear to be building up as $\epsilon \to 0.05$ are associated with the percolation transition (at $\epsilon = 0$) of the species-4 oxygen atoms, or the percolation of some subset of these atoms (e.g., the percolation of the "hard cores" described in Appendix B, Sec. C).

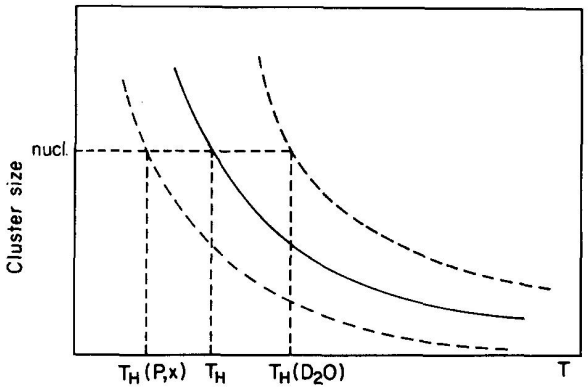

FIG. 8. Schematic dependence of the mean cluster volume on temperature, indicating the relation $T_s \lesssim T_H$ that one would expect if the Angell singularity temperature T_s were to correspond to a percolation transition (mean patch size = ∞). Since the homogeneous nucleation temperature T_H corresponds to an increase in the mean patch size to only a certain critical value, we expect T_H to be just slightly larger than T_s. Also shown are the corresponding curves for D_2O and for pressurized water. The model predicts that the effects of isotope dilution and pressure on T_s and T_H should be roughly the same (see discussion in Sec. VIIC).

Among the predictions are the following.

(a) For D_2O, T_s is slightly higher than for H_2O; this is confirmed by experimental data.[57]

(b) For pressures greater than atmospheric, T_s should decrease; this is also observed.[45]

(c) T_s should decrease in the presence of small amounts of a "patch-breaking impurity"; the probable validity of this prediction is suggested by very recent data.[57]

(d) The percentage decrease with pressure of T_s should *exceed* the corresponding percentage decrease with pressure of T_m, since the former has a built-in "amplification mechanism" arising from the fact that $f_4 = p_B^4$; this mechanism is not related to the factors determining the pressure dependence of T_m.

(e) T_s should take on a value just slightly smaller than T_H, the homogeneous nucleation temperature. The reason is illustrated in Fig. 8: as T decreases, the mean size of the "locally structured patches" increases monotonically, appearing to diverge at the percolation threshold f_4^c (roughly 0.35 for the ice lattice[40]). Since $f_4 = p_B^4$, and p_B increases roughly linearly with decreas-

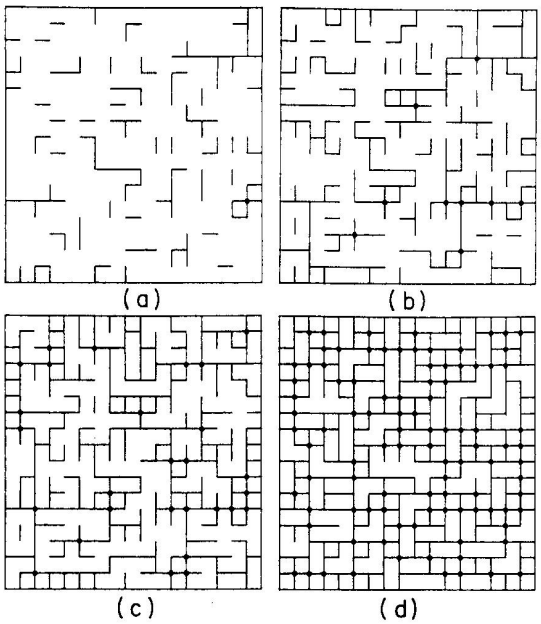

FIG. 9. Four simulations of random-bond percolation at four different values of bond probability p_B: (a) $p_B = 0.2$, (b) $p_B = 0.4$, (c) $p_B = 0.6$, and (d) $p_B = 0.8$. For simplicity of presentation, the simulations are given not for the three-dimensional ice I_h lattice, but rather for the two-dimensional square lattice (cf. Ref. 40). Also illustrated is the partitioning of the "oxygen atoms" into two species, those with four intact bonds (shown as black dots), and those with less than four intact bonds. Note that on the level of bond connectivity, there is an infinite bond cluster for $p_B > p_B^c$ ($= 0.5$). However, on the level of site connectivity, there is no infinite cluster until $f_4 = (p_B)^4$ exceeds the correlated-site threshold $f_4^c = 0.56$ (Ref. 40). Hence even at $p_B = 0.8$, when almost all the oxygen atoms belong to a single "infinite gel molecule," the four-bonded oxygens still form a set of *isolated* finite-size clusters since $f_4 = 0.4096$.

ing temperature, at a temperature only slightly above T_s, the size of a locally structured patch passes through the critical size for homogeneous nucleation. This prediction is in fact borne out quite nicely by experimental data: not only is T_s only a few degrees lower than T_H, but this relation *continues to hold* for pressures up to about 2 kbars, as both quantities decrease by roughly 50 °C in value. [93]

(f) If we extrapolate experimental data on the global mass density $\bar{\rho}(T)$ from the lowest measured value (at $T = -35$ °C) to $T = T_s$, the value obtained should be well above that of ice (which presumably has $f_4 \cong 1$), since f_4 is less than 1 at the percolation threshold. This is also found: extrapolation of the best available data on both H_2O and D_2O gives values significantly above ice density[94] at the respective values of T_s. Incidentally, if we evaluate $\bar{\rho}(T = T_s)$ using Kell's[44] empirical formula—based on extremely accurate measurements above T_m—we obtain the value 0.94, also well above the density of ice at -45 °C.

(g) If someone could ever make measurements for values of the reduced temperature *much* smaller than 0.05, we predict that the static quantities would cease their apparent divergences, while the dynamic quantities might indeed display a true singularity.

ACKNOWLEDGMENTS

We are deeply indebted to many individuals in connection with the present work. In particular, C. A. Angell kindly made available extensive unpublished results and enlightened us on many important ideas that we failed initially to appreciate. Virtually every point of this manuscript was discussed with P. Papon. J. Leblond, and C. A. Angell; we gratefully acknowledge their many useful suggestions and constructive criticisms. Conversations with P. G. de Gennes also helped us clarify our ideas considerably. Useful discussions are also acknowledged with S. Alexander, M. Azbel, L. Bosio, E. G. D. Cohen, M. H. Cohen, A. Coniglio, H. S. Frank, A. Geiger, G. Grest, J. Herzfeld, J. Imry, W. Känzig, W. Klein, D. Levesque, T. C. Lubensky, C. Mitescu, P. Pfeuty, P. Pincus, S. Redner, P. J. Reynolds, R. Speedy, D. Stauffer, F. H. Stillinger, and A. Voronel. G. Shlifer kindly wrote the computer program used to construct the simulations displayed in Figs. 5 and 9. Finally, one of us (H. E. S.) wishes to express his most sincere thanks to his colleagues in the *Laboratoire de Physique Thermique* for their warmth and kind hospitality during the period in which much of the present work was carried out. We also wish to thank two referees for their constructive criticism on the first version of this manuscript.

APPENDIX A: POTENTIALLY CONFUSING POINTS CONCERNING CORRELATED-SITE POLYCHROMATIC PERCOLATION

We have noted four potentially confusing points that frequently arise in presenting the model of Sec. 2. It is the purpose of this appendix to address each of these four points in turn. [95]

A. Bond connectivity vs site connectivity

The first potentially confusing point concerns the distinction between bond connectivity and site connectivity—more precisely, the distinction between (i) the formation of an infinite hydrogen bonded network at the bond percolation threshold, and (ii) the growth of the tiny patches of species-4 oxygens within this network.

Both phenomena can be illustrated with the same example, shown in Fig. 9. Suppose we have an infinitely high and infinitely long wire fence. Imagine also that a randomly chosen fraction p_B of the links of this fence are conducting, while the remaining fraction $q_B = 1 - p_B$ are insulating. Computer simulations of a finite (16×16) section of this imaginary fence are shown in Fig. 9 for $p_B = 0.2$, 0.4, 0.6, and 0.8.

(i) *Bond connectivity.* For p_B small, as in part (a), the system clearly consists of small cluster of conducting bonds. Most of the sites are isolated "monomers" and "dimers," with relatively few larger bond clusters. The system is said to be in its "sol" phase.

In (b) the conducting fraction p_B has doubled, yet the system still consists of only finite bond clusters ("polymers"). However, in (c), $p_B = 0.6$, and the system is

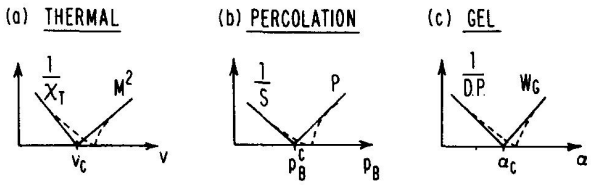

coupling constant	bond probability	"conversion"
$v_c = \tanh(J/kT_c)$	p_B^c = percolation pt.	α_c = gel point
droplet	bond cluster	polymer
M	P(p)	W_G = wt. fraction
χ_T	S(p)	D.P. = deg. of poly.
G(H,T)	$\langle N_{clusters} \rangle$	$\langle N_{molecules} \rangle$
Husimi-Temperley $d_+ = (2\beta+\gamma)/\nu = 4$	Fisher-Essam $d_+ = 6$	Flory $d_+ = 6$

FIG. 10. Illustration of the Frisch–Hammersley–de Gennes–Stauffer analogy (cf. Ref. 95) between (a) thermal phase transitions, (b) random-bond percolation, and (c) polyfunctional condensation. The top line identifies the corresponding meanings of the abscissas (and their critical values). The second line indicates the essential physical features, while the third line shows the corresponding "order parameter" and "order parameter response function." Next is shown the generating function, and finally the corresponding mean field theories (valid for systems with dimensionality d above a critical value d_+) are shown.

macroscopically quite different in nature: in addition to the finite clusters, there is a single cluster that is infinite in spatial extent. For some value of p_B in between part (b) and (c), there is a threshold p_B^c. Below p_B^c, the fence cannot conduct, while above p_B^c it can. Thus its *macroscopic* properties change suddenly as a microscopic parameter p_B increases infinitesimally from $p_B^c - \delta$ to $p_B^c + \delta$. The actual value of p_B^c depends strongly on the dimensionality of the system and even on the actual lattice; for the two-dimensional square lattice, $p_B^c = 0.5$ (exactly),[95] while for the three-dimensional ice I_h lattice, $p_B^c \cong 0.39$.[79]

The "connectivity" phase transition occurring at p_B^c has attracted much attention, in part due to intriguing analogies with ordinary "thermal" phase transitions (cf. Fig. 10), and in part because of its potential utility[95] in describing gelation of polyfunctional monomers (one can imagine each of the vertices of Fig. 9 is a four-functional monomer, and the bonds are chemical bonds).

(ii) *Site connectivity.* In the random-bond connectivity problem described previously, bonds are randomly chosen to be either black (with probability p_B) or white (with probability $q_B \equiv 1 - p_B$). One can clearly define a converse problem, the random-site problem, in which the sites are randomly chosen to be either black (with probability p_s) or white (with probability $q_s \equiv 1 - p_s$). The random-site problem will have a percolation threshold that is highly analogous to the percolation threshold exhibited in the random-bond problem, though the threshold value p_s^c will in general be different than p_B^c.

(iii) *Previous applications of bond connectivity to water.* Statements that water is a "gel" are equivalent to the statement that the connectivity of the oxygen atoms is above the bond percolation treshold. Bond percolation thresholds are not known with much accuracy for three-dimensional continuum systems, but it is widely believed that for a close-packed three-dimensional system, p_B^c would be comparable to its value for an fcc lattice, about 0.12. Molecular dynamics calculations on water indicate that p_B^c is in fact remarkably close to 0.39, its value for an ice I_h lattice. It is important to emphasize that water is probably above its bond percolation threshold[29]; the novel aspect of the present model does not concern bond connectivity, but rather the sort of site connectivity to be expected for the sites making up the infinite bond network.

B. Random-site percolation vs correlated-site percolation

Any study of the connectivity of two species of sites is termed a "site percolation problem." In Sec. A, we considered the simplest case, random-site percolation. Suppose the positions of the sites are not random, but are correlated. For example, if the system in question is an Ising ferromagnet, then the sites can represent Ising spins, with an "up spin" being black and a "down spin" being white. Of course, at infinite temperature the connectivity of the Ising spin system is identical to that of random-site percolation. At any finite temperature, however, the existence of a ferromagnetic exchange interaction energy J between nearest-neighbor spins will encourage neighboring spins to be parallel (i.e., neighboring sites to be of the same color). Because of the lattice-gas model of a fluid, correlated-site percolation has been found to be useful in describing solvent effects on gelation.[96]

An altogether different fashion of partitioning sites into two colors is that described in Sec. II. This procedure may be illustrated with Fig. 9, the random-bond percolation problem. Every site with four conducting bonds is colored black, and the remaining sites are white. Since the bonds are placed randomly, the fraction of four-bonded "black" sites is simply $f_4 = p_B^4$ [cf. Eq. (2.1)]. Hence (a) f_4 is quite small unless p_B is rather large (well above the bond percolation threshold), and (b) there is an amplification mechanism in the dependence of the concentration f_4 of black sites on the bond probability p_B: a 1% increase in p_B leads to a 4% increase in p_B^4. For example, $f_4 = 0.1296$ when p_B is 0.6 [Fig. 9(c)], while when $p_B = 0.8$, $f_4 = 0.4096$, [Fig. 9(d)]. The reader may verify by direct counting that roughly 13% and 41% of the sites are black, respectively.

Although the total number of four-bonded black sites is determined by simple considerations of random probability, the *spatial positions* (and hence the connectivity) of the black sites *are far from random.* Rather there is a distinct tendency for the black sites to have a "ferromagnetic" correlation and the resulting clusters are far less ramified than in random-site percolation. Accordingly, there is no meaning to the parameter p_s (site probability) since the probability of a site being black depends on the color of its four neighbors. The corresponding correlated-site percolation threshold is slight-

ly reduced from its value for the random-site problem: for the two-dimensional square lattice, $p_s^c \cong 0.59$, while $f_4^c \cong 0.56$[40]; for the three-dimensional ice I_h lattice, $p_s^c = 0.42$ while $f_4^c \cong 0.35$.[40]

C. Bichromatic vs polychromatic percolation

In Sec. A, we partitioned the sites of Fig. 9 into two distinct categories; black sites had four intact bonds, while the remaining sites were colored white. This is termed a bichromatic site percolation problem.

One can equivalently partition the sites of Fig. 9 into five distinct categories, black sites having four bonds, "blue" sites having three bonds, "red" sites having two bonds, etc. The problem posed by the connectivity of the five separate species is termed a polychromatic percolation problem.[97] Although most of this manuscript concerns bichromatic percolation, the full polychromatic percolation problem may be necessary for understanding some features of liquid water (cf. Appendix B, Secs. A and B).

D. Species correlations vs connectivity correlations

Several workers have called to our attention the following apparent paradox.[98] By definition, the color of a given site A depends only on the number of bonds incident upon that site. Hence although the color of site A is very strongly correlated with the colors of its four nearest-neighbors, it is completely independent of the color of its next nearest neighbors. Suppose we define the "two-site correlation function" $g_{ss}(r)$ to be the conditional probability that if a site at the origin is black, another site a distance r from the origin is also black. This function will not become long-range at the percolation threshold.

In percolation, one studies the connectivity correlation function or "pair connectedness" $\tilde{g}_{ss}(r)$, which is related to the conditional probability that if a site at the origin is black, another site a distance r from the origin is not only black but is also *connected* to the site at the origin by a path consisting of nearest-neighbor pairs of black sites. It is $\tilde{g}_{ss}(r)$ that becomes long-range at the percolation threshold and is substantially increased as the result of the correlation. Of course, it is the sharp increase in range of $\tilde{g}_{ss}(r)$, not $g_{ss}(r)$, that is responsible for patch formation.

APPENDIX B: A QUANTITATIVE EXAMPLE

It is instructive to show that quantitative comparison with experimental data can be obtained using a relatively simple—albeit somewhat rough—procedure. Specifically, we shall assume that the statics is dominated by the tiny patches of species-4 oxygens, while the dynamics is governed by species-0 and species-1 oxygens. Of course, all species play some role—these assumptions are made to simplify the quantitative calculations (other simplifying assumptions were tried; these were optimal).

In particular, it is possible using percolation theory to calculate the mean size of the tiny patches of four-bonded oxygen atoms as a function of p_B. One finds that these patches are remarkably small for *all* values of p_B except these extremely close to the percolation threshold.[39,40,89,99]

A. Anomalous contribution K_T^A to the isothermal compressibility

We first consider a local quantity, the volume per oxygen atom, $\tilde{V}_j$. It is plausible that $\tilde{V}_j$ depends on the number of bonds j emanating from that atom, with

$$\tilde{V}_0 \lesssim \tilde{V}_1 \lesssim \tilde{V}_2 \lesssim \tilde{V}_3 \lesssim \tilde{V}_4 \,. \tag{B1}$$

Suppose we now partition the system into cells of characteristic dimension L, where L is typically a few nearest-neighbor distances. With each cell we associate a *local* density ρ_L, and we study the fluctuations of this local density from cell to cell. Since the positions of each species are correlated and since the density is related to the site species by Eq. (B1), the density *fluctuations* are correlated. That is, they are quite different in character from the density fluctuations in the corresponding random-site model consisting of the same five species, present in the same mole fractions. The isothermal compressibility in this correlated-site percolation problem is enhanced, just as the isothermal compressibility in a van der Waals gas is enhanced relative to its value in an ideal gas.

We can readily calculate the anomalous contribution K_T^A to density fluctuations due to species-4 patches. For the sake of illustration, we first neglect the correlations. We can readily evaluate the mean square of the density fluctuations, considering the volume per oxygen atom of Eq. (B1). For convenience, we also suppose that $\tilde{V}_4 = \tilde{V}_{\rm ice}$ and that the volume per oxygen atom for the remaining four species assume roughly the same value, which we shall call $\tilde{V}_{\rm gel}$ (referring to the "rest of the gel"). To evaluate $\tilde{V}_{\rm gel}$, we note that $\bar{\rho}(T)$ has an inflection point at roughly 100 °C, and hence we take for $\bar{\rho}_{\rm gel}$ a straight line tangent to $\bar{\rho}(T)$ for $T = 100$ °C. Using data of Kell,[44] we find

$$\bar{\rho}_{\rm gel} = (1218 - 0.695\,64T)\,{\rm kg\,m^{-3}} \,, \tag{B2}$$

where T is measured in K. We can now evaluate p_B using measured values of $\bar{\rho}(T)$ between -30 and $+50$ °C, since

$$p_B = [(\bar{\rho}_{\rm gel} - \bar{\rho})/(\bar{\rho}_{\rm gel} - \rho_4)]^{1/4} \,. \tag{B3}$$

The result of this calculation is shown in Fig. 11, and agrees surprisingly well with various estimates in the literature based, e.g., on Raman and infrared spectroscopic studies.[36,37] For future "order-of-magnitude" calculations, it is convenient to represent the curve $p_B(T)$ of Fig. 11 by the simple linear approximation.

$$p_B = 1.8 - 0.004T \,, \tag{B4}$$

with T the absolute temperature.

The fraction p_B^4 of four-bonded oxygens with local density ρ_4 contributes to the density fluctuations $\overline{(\delta\rho)^2}$ a term $p_B^4(\rho_4 - \bar{\rho})^2$. The remaining fraction $(1 - p_B^4)$ with mean density $\bar{\rho}_{\rm gel}$, contributes a term $(1 - p_B^4)(\bar{\rho}_{\rm gel} - (\delta\rho)^2$ Hence

$$\overline{(\delta\rho)^2} = p_B^4(\rho_4 - \bar{\rho})^2 + (1 - p_B^4)(\bar{\rho}_{gel} - \bar{\rho})^2$$
$$= p_B^4(1 - p_B^4)(\rho_4 - \bar{\rho}_{gel})^2 , \quad \text{(B5)}$$

where the second equality follows from Eq. (B3), written in the equivalent form $\bar{\rho} = p_B^4\rho_4 + (1 - p_B^4)\bar{\rho}_{gel}$. The function $V\overline{(\delta\rho)^2}/(\bar{\rho}^2 k_B T)$ is plotted in Fig. 12. It is clear that the essential features of the observed temperature dependence of K_T^A are displayed. Note also that the predicted maximum is certainly in a temperature region without physical significance. The magnitude of K_T^A is smaller than the total observed value of K_T, but the inclusion of correlations will of necessity serve to increase the density fluctuations.

B. Isotope effect: effect of D_2O substitution

Suppose we repeat the calculation leading to Eq. (B4) for the isotope D_2O, for which extremely accurate density data exist.[44] We find that Eq. (B4) is replaced by

$$p_B = 1.845 - 0.004T . \quad \text{(B6)}$$

It is a useful check on the percolation picture to compare Eq. (B4) for H_2O and Eq. (B6) for D_2O. We see that at $T = 273$ K, p_B is about 5% larger for D_2O than for H_2O. This is quite reasonable. Indeed, the latent heats for D_2O are roughly 5% larger than for H_2O (presumably both effects have a common physical origin, a lower zero-point motion of the deuteron relative to the proton).

It would be particularly valuable to have accurate experimental data for two-component mixtures of H_2O and D_2O, since the detailed predictions of the model (some vary as p_B^4) could then be tested.

C. Comparison between the density fluctuations and the entropy fluctuations

One empirical fact that at first sight may seem somewhat mysterious is that the "anomalous" density fluctuations begin to manifest themselves at temperatures considerably higher than the temperatures at which the entropy fluctuations show up. For example, K_T^A begins to increase when T is lowered below 46 °C, while C_P does not begin to increase sharply until T is below T_m.[1,3] Two possible explanations for this behavior immediately suggest themselves. (i) There are temperature-dependent "background" terms that differ[65] for the two cases in question, K_T and C_P. (ii) Patches of rather larger spatial extent are necessary to give rise to a *significant* entropy difference between what is seen by a Maxwell demon located inside a patch and another Maxwell demon not located in a patch. For example, it is plausible that the density fluctuation caused by a two-site patch is significant, while the corresponding entropy fluctuation is not.

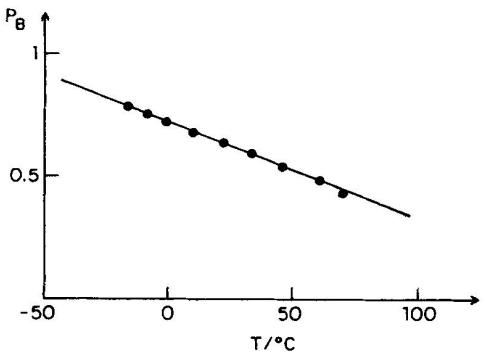

FIG. 11. Dependence on temperature of the bond probability predicted by the analysis described in the text. Also shown as a solid curve is the convenient approximation of Eq. (B4), which is used in the numerical calculations of Appendix B. The qualitative form obtained is consistent with proposals based on spectroscopic data (cf., e.g., Refs. 36 and 37). In particular, the prediction that p_B continues to vary smoothly with T even for $T < T_m$ agrees with previous work (Refs. 1, 65, and 83).

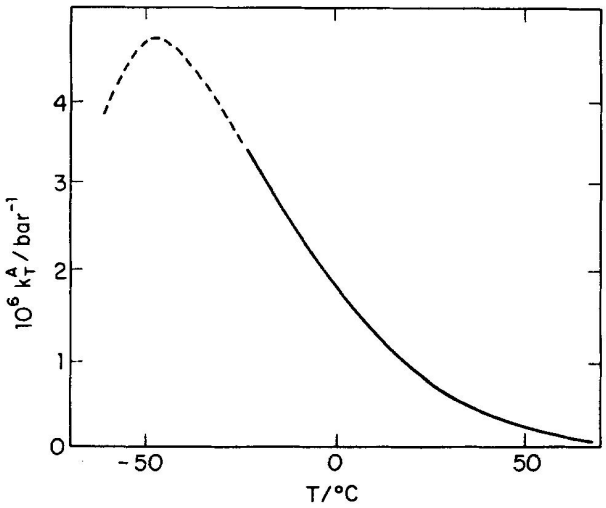

FIG. 12. Schematic temperature dependence of K_T^A, the anomalous contribution to the isothermal compressibility due to the presence of tiny patches for four-bonded oxygens, as calculated using the approximations of Eqs. (B2), (B4), and (B5). The dashed line indicates the predictions in the temperature region for which no data exist. There is some recent evidence (Ref. 51) that, by dilution of pure H_2O with an optimal amount of patch-breaking impurity, K_S can in fact be made to undergo a maximum.

The second explanation is particularly physical, since it explains the remarkable sensitivity of the C_P anomaly to even the most minute quantities[57] of a second component ("patch-breaking" impurity). In fact, it could well be that one should redefine the term "patch" when discussing the entropy. For example, one might wish to consider an "entropy-fluctuation" patch as made up only of species-4 oxygens, all of whose *neighbors* are also species 4. We call such patches "hard cores," since they are obtained for the original patches by removing all the border sites. Clearly, at a given temperature (i.e., at a given value of p_B), the mean size and number of such "hard cores" is considerably smaller than the corresponding values for the original clusters of species-4 oxygens.

D. Order-of-magnitude estimates for the low-temperature entropy of liquid water

Here we discuss in more detail the curve drawn qualitatively in Fig. 7 for the entropy $S_{NL}(T)$ of a "normal liquid" (what water might be like were there no species-

4 patches). To evaluate $S_{NL}(T)$, we must subtract from the *total* specific heat C_P the part C'_P that can be attributed to the existence of the species-4 patches—since these are presumably responsible for the decrease of the entropy from $S_{NL}(T)$ to $S_W(T)$. Thus we may define

$$C_{NL} = C_P - C'_P . \tag{B7}$$

Clearly C'_P is some fraction of the total configurational specific heat, which in turn is roughly half the total specific heat in the region between 0 and 100 °C.[3] Hence we anticipate that C_{NL} may be bounded as follows:

$$9 \text{ cal mol}^{-1}\text{K}^{-1} \leq C_{NL} \leq 18 \text{ cal mol}^{-1}\text{K}^{-1} . \tag{B8}$$

In order to calculate $S_{NL}(T)$, we would need to know the complete temperature dependence of C_{NL} for all T. It is interesting to calculate the implications of choosing a temperature-independent value between the upper and lower bounds of Eq. (B8), say $C_{NL}(T) = 14$ cal mol^{-1} K^{-1}.

The entropy $S_{NL}(T)$ may be then evaluated using the thermodynamic identity

$$S_{NL}(T) = S_{NL}(T = 173 \text{ K}) + \int_{173}^{T} C_{NL}(T')\, d(\ln T') . \tag{B9}$$

Here $S_{NL}(T = 173$ K) represents the entropy at $T'_m = -100$ °C, which in turn may be estimated by adding the entropy of fusion $S_F = 5.3$ cal mol^{-1} K^{-1} to the entropy of ice at T'_m. Thus we find

$$S_{NL}(T) = \left[5.3 + 5.2 + 14 \log\left(\frac{T}{173}\right)\right] \text{cal mol}^{-1}\text{K}^{-1} . \tag{B10}$$

From Eq. (B10) we may estimate the intercept T'_0 of $S_{NL}(T)$ with $S_x(T)$, the entropy of ice; we find $T'_0 = 101$ K. Similarly, we may estimate the intercept T_1 of $S_{NL}(T)$ with $S_W(T)$, the entropy of water; we find $T_1 = 611$ K. These two estimates are quite plausible, in light of the fact that the "normal liquid" (water without the patches) would presumably undergo a glass transition at $T_g = 140$ K, while the patches are certainly absent near the critical temperature ($T_c = 647$ K).

In order to test the sensitivity of this very rough calculation to the assumption concerning the value $C'_P(T)$, we can repeat the above steps for the choice $C_{NL}(T) = 13$ cal mol^{-1} K^{-1}. We find $T'_0 = 97$ K, and $T_1 = 492$ K. Thus T'_0 is not very dependent on the value chosen, while T_1 is. (Thus T_1 has rather huge error bars, but in any case even 492 K is in a temperature region in which comparatively few species-4 patches should exist.)

E. Dynamic properties of low-temperature water

A comparatively small fraction of the total work on the theory of water concerns itself with quantitative calculations of dynamic properties. Accordingly, even rather crude arguments may afford some utility.

In this section, we demonstrate that quantitative agreement with experimental data for the self-diffusion coefficient D_s may be obtained by regarding transport as arising from the "mobile" fraction of Eq. (6.1), with $A = B = 1$ for simplicity. It is of interest that the same probability function $p_B(T)$ obtained in (B4) above is sufficient to describe the dynamics. This agreement is mitigated by the fact that there is one adjustable parameter, the characteristic hydrogen bond lifetime τ_{HB}.

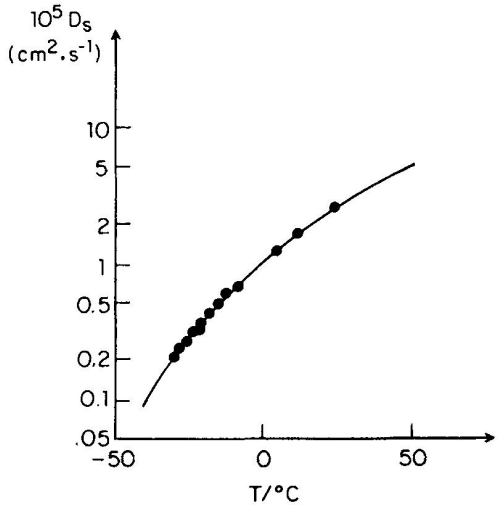

FIG. 13. Illustration of the degree of agreement between the experimental data of Ref. 71 on the coefficient of self-diffusion D_s and the predictions of Eqs. (B14) and (B4). We emphasize that there is a second parameter in (B14) not present in the static calculations: the characteristic bond lifetime τ_{HB}. The fact that the choice of this parameter that best fits the data is of the correct order of magnitude is encouraging (cf. Ref. 68, and references therein).

Thus far, our discussion has concerned the static properties of liquid water—each computer simulation corresponds to a snapshot of the system with a shutter speed much shorter than τ_{HB}. Suppose we make l separate compute simulations and regard these as corresponding to l separate snapshots, each separated in time by an interval τ_{HB}. This is an extremely crude picture of dynamics, since it neglects any possible "memory" effects. Nevertheless, it is interesting to note that it provides a model sufficiently simple that quantitative calculations can be carried out with only one adjustable parameter (τ_{HB}) and that the agreement with experimental data is quite encouraging.

Suppose that during the time interval τ_{HB}, the "mobile" fraction F_M given by (6.1) is available for transport. The fraction of "immobile" atoms, F_I, is given by

$$F_I \equiv 1 - F_M = 1 - (f_0 + f_1) = f_2 + f_3 + f_4 . \tag{B11}$$

The probability of randomly chosen oxygen to be immobile in a given realization is thus F_I, while the probability that this oxygen remains immobile for *two* successive realizations is F_I^2. In general, the probability of a randomly chosen oxygen to remain immobile for l realizations is F_I^l. However, $l\tau_{HB}$ is a measure of the "total immobility" of this oxygen,and thus of the rotational relaxation time τ_R (as measured, e.g., by dielectric relaxation experiments). Hence we can write

$$F_I^l = F_I^{\tau_R / \tau_{HB}} = \tfrac{1}{2} , \tag{B12}$$

where the probability $\frac{1}{2}$ is only a numerical constant. Thus (B12) provides a simple and physically plausible equation relating the characteristic rotational relaxation time to the hydrogen bond probability,

$$\tau_R = (\tau_{HB} \ln \tfrac{1}{2}) / \ln F_I . \tag{B13}$$

The most accurate experimental data are not for τ_R but rather for the coefficient of self-diffusion D_s. Pruppacher[72] has noted that the two quantities are inversely related, to a good approximation, with $D_s\tau_R \cong 2.11\times10^{-16}$ cm^2. Hence (B13) becomes

$$D_s = (-3.04\tau_{HB}^{-1}\ln F_f)\times10^{-16}\ \text{cm}^2\,\text{sec}^{-1}\ . \qquad \text{(B14)}$$

Very little is known about the mean bond lifetime τ_{HB}, but there are some data[68] suggesting that τ_{HB} depends sufficiently weakly on T that we may to first approximation neglect its temperature dependence. Then we have in Eq. (B14) a closed-form expression for D_s with only one adjustable parameter, τ_{HB}. Figure 13 demonstrates the degree of agreement between (B14) and experiment[71] that may be obtained on choosing $\tau_{HB} = 2.3$ psec. It is gratifying that the value of τ_{HB} that emerges from our analysis is comparable with estimates of τ_{HB} based on experiment (cf., e.g., Ref. 68, and references therein).

An additional test of Eq. (B14) would be to make accurate measurements of both D_s and τ_{HB} for the isotope D_2O; Eqs. (B4) and (B6) predict that the product $D_s\tau_{HB}$ should be substantially larger for D_2O than for H_2O.

[1]C. A. Angell, in *Water: A Comprehensive Treatise*, edited by F. Franks (Plenum, New York, 1981), Vol. 7, and references therein.
[2]H. E. Stanley, J. Phys. A **12**, L329 (1979).
[3]D. Eisenberg and W. Kauzmann, *The Structure and Properties of Water* (Oxford University, New York, 1969).
[4]N. H. Fletcher, Rep. Prog. Phys. **34**, 913 (1971).
[5]R. A. Horne, ed., *Water and Aqueous Solutions* (Wiley-Interscience, New York, 1972).
[6]F. Franks, ed., *Water: A Comprehensive Treatise* (Plenum, New York, 1972), Vol. 1.
[7]A. Ben-Naim, *Water and Aqueous Solutions* (Plenum, New York, 1974); *Hydrophobic Interactions* (Plenum, New York, 1980).
[8]J. W. Perram and L. Levine, Adv. Mol. Relaxation Processes **6**, 85 (1974).
[9]F. H. Stillinger, Adv. Chem. Phys. **31**, 1 (1975).
[10]S. A. Rice, Topics in Current Chemistry **60**, 109 (1975).
[11]W. C. Roentgen, Ann. Phys. **45**, 91 (1892).
[12]G. Némethy and H. A. Scheraga, J. Chem. Phys. **36**, 3382, 3401 (1962); **41**, 680 (1964).
[13]H. S. Frank, Science **169**, 635 (1970).
[14]A. T. Hagler, H. A. Scheraga, and G. Némethy, J. Phys. Chem. **76**, 3229 (1972).
[15]G. M. Bell, J. Phys. C **5**, 889 (1972).
[16]B. R. Lentz, A. T. Hagler, and H. A. Scheraga, J. Phys. Chem. **78**, 1531 (1974).
[17]M. S. Jhon and H. Eyring, Annu. Rev. Phys. Chem. **27**, 45 (1976).
[18]P. H. Meijer, R. Kikuchi, and P. Papon, Phys. Rev. A (submitted for publication); P. H. Meijer, R. Kikuchi, and E. van Royen, Phys. Rev. A (submitted for publication).
[19]W. Kauzmann, in *L'Eau et les Systèmes Biologiques*, edited by A. Alfsen and A. J. Berteaud (Editions du Centre National de la Recherche Scientifique Paris, 1976), p. 63.
[20]J. D. Bernal and R. H. Fowler, J. Chem. Phys. **1**, 515 (1933).
[21]J. A. Pople, Proc. R. Soc. London A **205**, 163 (1951); J. D. Bernal, *ibid.* **280**, 299 (1964).
[22]C. A. Angell, J. Phys. Chem. **75**, 3698 (1971).
[33]J. H. Gibbs, C. Cohen, P. D. Fleming, and H. Porosoff, J. Solution Chem. **2**, 277 (1973).
[24]R. Alben and P. Boutron, Science **187**, 430 (1975).
[25]M. G. Sceats, M. Stavola, and S. A. Rice, J. Chem. Phys. **70**, 3927 (1979).
[26]M. G. Sceats and S. A. Rice, J. Chem. Phys. **72**, 3236, 3248, 3260, 6183 (1980).
[27]M. G. Sceats and S. A. Rice, in Ref. 1.
[28]F. H. Stillinger, Philos. Trans. R. Soc. London B **278**, 97 (1977).
[29]A. Geiger, F. H. Stillinger, and A. Rahman, J. Chem. Phys. **70**, 4185 (1979).
[30]A. Rahman and F. H. Stillinger, J. Chem. Phys. **55**, 3336 (1971).
[31]F. H. Stillinger and A. Rahman, J. Chem. Phys. **57**, 1281 (1972).
[32]A. Rahman and F. H. Stillinger, J. Am. Chem. Soc. **95**, 7943 (1973).
[33]F. H. Stillinger and A. Rahman, J. Chem. Phys. **60**, 1545 (1974).
[34]D. W. Wood, in *Water: A Comprehensive Treatise*, edited by F. Franks (Plenum, New York, 1979), Vol. 6.
[35]We shall speak of a bond between two water molecules as being in either of two states, intact or broken. This imposition of a discrete symmetry on a physical function, the interparticle potential, which is certainly anything but discrete, is an assumption. However, it is not unlike that made in the lattice-gas model, which has been found to be adequate for describing fluid phenomena near the critical point. Moreover, we can imagine the discrete symmetry being imposed even on a physical picture of "bent" bonds in which bonds bent more than some some cutoff angle θ_{HB} are regarded as being "broken" (Refs. 26 and 27).
[36]W. A. P. Lück, Discuss. Faraday Soc. **43**, 115 (1967); in *Membrane Methods in Water and Waste Water Treatment*, edited by G. Delfort (Academic, New York, 1979). See also W. A. P. Lück and W. Ditter, Z. Naturforsch. **24**, 482 (1969); J. Phys. Chem. **74**, 3687 (1970).
[37]G. E. Walrafen, in Ref. 6, and references therein.
[38]This assumption is supported by the finding in Ref. 29 that the percolation threshold for ST2 water agrees with that for the ice I_h lattice (cf. Appendix A, Sec. B).
[39]A. Geiger, *et al.* (work in progress).
[40]Extensive Monte Carlo simulations have been carried out for two different lattices, each with coordination number $z=4$. For the $d=2$ square lattice, statistics were obtained for systems with up to $(300)^2=90\,000$ sites [R. L. Blumberg, G. Shlifer, and H. E. Stanley, J. Phys. A. **13**, L147 (1980)]. For the $d=3$ ice I_h lattice, Monte Carlo simulations were carried out for systems up to $(22)^2 44 = 21\,296$ sites [R. L. Blumberg *et al.* (unpublished results)].
[41]See, e.g., O. K. Rice, *Statistical Mechanics Thermodynamics and Kinetics* (Freeman, San Francisco, 1967), p. 232 or H. E. Stanley, *Introduction to Phase Transitions and Critical Phenomena* (Oxford University, New York, 1971) p. 97.
[42]H. S. Frank, in Ref. 6, p. 515.
[43]R. J. Speedy and C. A. Angell, J. Chem. Phys. **65**, 851 (1976).
[44]G. S. Kell, J. Chem. Eng. Data **20**, 97 (1975). Analogous data for D_2O are presented in G. S. Kell, *ibid.* **12**, 66 (1967).
[45]H. Kanno and C. A. Angell, J. Chem. Phys. **70**, 4008 (1979).
[46]J. Rouch, C. C. Lai, and S. H. Chen, J. Chem. Phys. **65**, 4016 (1976).
[47]J. Teixeira and J. Leblond, J. Phys. (Paris) Lett. **39**, L83 (1978).
[48]E. Trinh and R. Apfel, J. Acoust. Soc. Am. **63**, 777 (1978).
[49]J. C. Bacri and R. Rajaonarison, J. Phys. (Paris) Lett. **40**, L403 (1979).
[50]R. T. Lagemann, L. W. Gilley, and E. G. McLeroy, J. Chem. Phys. **21**, 819 (1953).

[51]We are grateful to Professor H. S. Frank, Dr. A. Geiger,

and Professor W. Kauzmann for clarifying for us the distinction between the two classes of impurities discussed here. In particular, Professor Frank has proposed an argument based on the Le Chatelier principle which correctly predicts the effect of the second type of impurity [H. S. Frank (private communication)]. A careful experimental study of the effect of patch-breaking impurities on compressibility is underway [J. M. Alloneau, B. Jugue, O. Conde, and J. Teixeira (unpublished results)]; see also Refs. 1 and 57. Work on the second class of impurities includes H. S. Frank and M. W. Evans, J. Chem. Phys. **13,** 507 (1945); B. B. Benson and D. Krause, *ibid.* **64,** 689 (1976); A. Geiger, A. Rahman, and F. H. Stillinger, *ibid.* **70,** 263 (1979); C. Pangali, M. Rao, and B. J. Berne, *ibid.* **71,** 2975, 2982 (1979).

[52]See, e.g., L. L. D. Landau and E. M. Lifschitz, *Statistical Physics*, 2nd ed. (Pergamon, London, 1969), p. 351.

[53]Martinetti, quoted in *Handbook of Physics and Chemistry*, C.R.C. (1890).

[54]M. A. Anisimov, A. V. Voronel', N. S. Zaugol'nikova, and G. I. Ovodov, JETP Lett. **15,** 317 (1972).

[55]C. A. Angell, J. C. Shuppert, and J. C. Tucker, J. Phys. Chem. **77,** 3092 (1973).

[56]D. H. Rasmussen, A. P. MacKenzie, C. A. Angell, and J. C. Tucker, Science **181,** 342 (1973).

[57]M. Oguni and C. A. Angell, J. Chem. Phys. **73,** 1948 (1980).

[58]R. A. Fine and F. J. Millero, J. Chem. Phys. **63,** 89 (1975).

[59]B. V. Zheleznyi, Russ. J. Phys. Chem. **42,** 950 (1968); **43,** 1311 (1969).

[60]H. Kanno and C. A. Angell, J. Chem. Phys. **73,** 1940 (1980).

[61]C. A. Angell and H. Kanno, Science **193,** 1121 (1976).

[62]R. Vedam and G. Holton, J. Acoust. Soc. Am. **43,** 108 (1968).

[63]C. A. Angell, J. Chem. Educ. **47,** 583 (1970).

[64]C. A. Angell and E. J. Sare, J. Chem. Phys. **52,** 1058 (1970).

[65]C. A. Angell (private communication).

[66]C. P. Johari, Philos. Mag. **35,** 1077 (1977).

[67]See, e.g., L. Pauling, *The Nature of the Chemical Bond*, 3rd ed. (Cornell University, Ithaca, 1960), Chap. 12.

[68]C. J. Montrose, J. A. Bucaro, J. Marshall-Croakley, and T. A. Litovitz, J. Chem. Phys. **60,** 5025 (1974).

[69]J. Hallett, Proc. Phys. Soc. London **82,** 1046 (1963).

[70]Yu. A. Osipov, B. V. Zheleznyi, and N. F. Bondarenko, Zh. Fiz. Khim. **51,** 1264 (1977).

[71]K. T. Gillen, D. C. Douglass, and M. J. R. Hoch, J. Chem. Phys. **57,** 5117 (1972).

[72]H. Pruppacher, J. Chem. Phys. **56,** 101 (1972).

[73]The orientational relaxation time of a dilute spin probe has been reported down to $T=-33°C$ by M. K. Ahn, J. Chem. Phys. **64,** 134 (1976).

[74]The nuclear spin-lattice relaxation time T_1 has been measured for protons in H_2O and for deuterons in D_2O as well as for the isotope ^{17}O (see, e.g., Table 6 of Ref. 1).

[75]Dielectric relaxation time data [C. H. Collie, J. B. Hasted, and D. M. Riston, Proc. R. Soc. London A **60,** 145 (1948)] thus far extend only to $T=-8°C$, but nevertheless are sufficient to indicate clearly a sharp increase with decreasing temperature.

[76]See Ref. 3, p. 223.

[77]F. A. Goncalves, "The Viscosity of H_2O+D_2O Mixtures in the Range 20°C–60°C" (preprint).

[78]C. A. Angell, E. D. Finch, L. A. Woolf, and P. Bach, J. Chem. Phys. **65,** 3063 (1976).

[79]The more modern methods of percolation theory have not yet been applied to the problem of random-bond percolation on the ice I_h lattice. However, an early estimate of $p_B^c=0.39$ is known from the Monte Carlo work of V. A. Vyssotsky, S. B. Gordon, H. L. Frisch, and L. M. Hammerlsey, Phys. Rev. **123,** 1566 (1961). The diamond lattice has been studied with much more accuracy, and $p_B^c=0.388\pm0.005$ is obtained from the low-density series expansion work of M. F. Sykes, D. S. Gaunt, and M. Glen, J. Phys. A **9,** 1705 (1976).

[80]We are currently extending our quantitative analysis to include effects due to nonrandom bonds. There are some indications that such "cooperative effects" may be important; see e.g., P. Barnes, J. L. Finney, J. D. Nicholas, and J. E. Quinn, Nature **282,** 459 (1979).

[81]F. H. Stillinger, "Water Revisited" (preprint). We are grateful to Dr. Stillinger for communicating his results to us prior to publication.

[82]Ref. 32 also gives f_0 and f_1.

[83]W. Lück (private communication).

[84]R. Bansil (private communication).

[85]J. Teixeira and S. H. Chen (unpublished results).

[86]P. A. Egelstaff, *An Introduction to the Liquid State* (Academic, New York, 1967).

[87]M. Sakamoto, B. N. Brockhouse, R. G. Johnson, and N. K. Pope, J. Phys. Soc. Jpn. **17,** Supplement B-II, 370 (1962).

[88]J. D. Irish, W. G. Graham, and P. A. Egelstaff, Can. J. Phys. **56,** 373 (1978).

[89]R. Blumberg *et al.* (unpublished results).

[90]L. Bosio *et al.* (work in progress); previous small-angle measurements are limited to $T>T_m$ [see, e.g., R. W. Hendricks, P. G. Mardon, and L. B. Shaffer, J. Chem. Phys. **61,** 319 (1974)].

[91]J. Dore, L. Bosio, and J. Teixeira (work in progress).

[92]J. Teixeira and S. H. Chen (work in progress).

[93]H. Kanno, R. J. Speedy and C. A. Angell, Science **189,** 880 (1975).

[94]See, e.g., N. H. Fletcher, *The Chemical Physics of Ice* (Cambridge University, Cambridge, England, 1970) and P. V. Hobbs, *Ice Physics* (Oxford University, London, England, 1974).

[95]An elementary introduction to the concepts of percolation theory may be found in H. E. Stanley, *Introduction to Phase Transitions and Critical Phenomena*, 2nd ed. (Oxford University, London and New York, 1981). Two recent technical reviews of percolation theory are D. Stauffer, Phys. Rep. **54,** 1 (1979) and J. W. Essam, Rep. Prog. Phys. (in press).

[96]A. Coniglio, H. E. Stanley, and W. Klein, Phys. Rev. Lett. **42,** 518 (1979).

[97]R. Zallen, Phys. Rev. B **16,** 1426 (1977).

[98]R. Speedy (private communication); W. Klein (private communication); A. Coniglio (private communication).

[99]*Note added in proof*, Subsequent to the completion (and submission) of the present work, we have learned that the model proposed in Ref. 2 and developed in Sec. 2 of the present manuscript has been successfully applied to a *solid-state* system, $aSiH_x$ (amorphous silicon hydride) by M. H. Brodsky [Solid State Comm. (in press)]. Specifically, Brodsky proposes that pure Si corresponds to our model of low-temperature water with $p_B=1$. Hydrogenation corresponds to breaking covalent Si–Si bonds, and therefore corresponds to increasing temperature, pressure, or patch-breaking impurity concentration. By doing calculations on the system of "disconnected Si patches," Brodsky succeeds in predicting the results of several hitherto unexplainable experiments. The following very recent work also provides additional support for the present model: Geiger (Ref. 39) has verified for ST2 water our assumption that the local density associated with a patch in the hydrogen-bonded network is less than the mean density.